Universitat de les Illes Balears

Master' Thesis

EXPLOSIVE TRANSITIONS IN SITE PERCOLATION.

Dianela A. Osorio Becerra.

Master's Degree in Physics of Complex Systems

At the Universitat de les Illes Balears (UIB) in collaboration with the Spanish National Research Council (CSIC). Organized and taught by IFISC (Institute for Cross-Disciplinary Physics and Complex). Palma de Mallorca, Spain.

Academic year 2019-2020

EXPLOSIVE TRANSITIONS IN SITE PERCOLATION.

Dianela A. Osorio Becerra.

Master´s Thesis

Postgraduate Studies Center

Universitat de les Illes Balears

Academic year 2019-2020

Keywords: Percolation, explosive percolation, critical threshold, order parameter, phase transition.

Master´s Thesis Supervisor: Pere Colet.

Master´s Thesis Supervisor and Director of the Master: Raúl Toral.

Contents

1 General description

Due to its simplicity and great application, it is known that percolation is one of the phenomena widely studied by statistical physics that addresses the theory of phase transitions and critical phenomena. In 2009 [1] the authors proposed a percolation variant introducing a competitive process between sites (or bonds), which prevents large clusters from joining each other, as a possible means of delaying the phase transition of a densely connected network, leading to explosive transitions or atypical and abnormal behaviors. This new type of percolation brought great interest, leading to a series of studies, among which the analysis of the order of the transition (continuous or discontinuous), the creation of others models with explosive behaviors, scale analysis, among others.

In this work we will study site percolation. As an algorithm to delay the transition and cause explosive percolation, we propose a variant of the sum rule proposed in [1] which we call global sum rule. In order to characterize the phase transition we will make use of numerical analysis. We explore the behavior of the transition for different order parameters, in the same way we evaluate the changes that the transition can undergo with different sizes and dimensions of the network, as well as for different number of tries in the global sum rule.

In order to facilitate the interpretation of results, this work is organized as follow: a chapter has been devoted to a brief review of basic concepts and that we consider most important. Then we present the results of our study, right here the graphs and results obtained are presented and analyzed, in order to give in another section the conclusions. Finally a list with the references given in the development of the text for those who want to go deeper into these topics.

2 Introduction.

To frame the reader in the foundations of our research, we will take this chapter to succinctly address just enough about the topic of classic percolation and explosive percolation, we refer the reader to [2, 3, 4, 5, 6, 7] for a more detailed study of these topics.

Since its introduction, percolation theory has been of great interest due to its simplicity and applicability [8]. Many studies are within the statistical mechanics framework and fundamentally on issues related to phase transitions and critical phenomena. From the classical percolation models the idea was that network connectivity that extends throughout the system occurs in a fluid and continuous manner. However, today it is known that there diverse types of percolation transitions [9]. A study that attracted a lot of attention was presented in reference [1] where researchers are found that in special cases, connectivity could emerge as an explosion, through a phenomenon they named "explosive percolation".

The connectivity formation can be understood as a phase transition. Phase transitions are omnipresent in nature, in general they are classified according to how the order parameter changes at the transition point [10], with a discrete jump (first order phase transition) or continuously (second order phase transition).

Phase transitions also provide a practical description of how individual sites or bonds in a random network gradually come together, one by one, through short-range connections over time. When the number of connections reaches a critical threshold, a phase change causes the largest cluster of sites to grow rapidly, resulting in super-connectivity.

In classical percolation, sites and pairs of sites are chosen at random to form connections, the probability that two clusters merge is proportional to their size, once a large cluster has formed, it dominates the system, absorbing any cluster smaller that could merge and grow. In explosive percolation, the network grows, but the growth of the large cluster is hindered, resulting in many large but disconnected clusters growing until the system reaches the critical threshold where adding only one additional bond or site induces an instantaneous change to the super-connectivity, all the large clusters combine at once in a single violent fusion.

In addition to the theoretical interest that this type of transitions has to understand the interaction between structure and dynamics, its practical consequences can also be very relevant.

2.1 Percolation.

The study of percolation is closely related to fundamental concepts such as phase transitions, critical phenomena, fractals, scaling, universality and renormalization [3, 4]. Percolation is a phenomenon of daily life, when studying percolation what you want is to see if a certain magnitude can flow through a system (what flows can be a fluid in a porous medium, the information through our connected devices to the Internet, infections or epidemics through a population, etc.), in general, it answers the questions that arise when considering the geometric connectivity of practically any type of object, so it constitutes an excellent model to apply in fields such as statistical physics, epidemiology, population dispersion, etc [11].

2.2 General percolation model.

A practical way of studying the phenomenon of percolation is from graphs. A graph is considered an idealized random medium in two or more dimensions, so the simplest model that we can imagine in percolation that presents interesting behavior is a two dimensional lattice (although the model can be extended to other networks), where it is considered that a stimulus carried out at one end of the network must be reproduced in its entirety at the other end. If this connectivity is carried out by the edges it is called bond percolation, while if it is determined by the nodes it is known as site percolation (see figure 1 (a) and (b)). Usually, the path followed by which the stimulus flows through bonds (or sites) is called percolating trajectory. These trajectories have different lengths and are determined by the number of occupied sites or bonds.

In site percolation, a set of N points forming a lattice is considered, each site can be occupied or empty, a site is connected to its neighbors if they are also occupied. In the case of bond percolation, all sites are present, but there are only bonds between them with a certain probability r, if $r = 1$ all nodes are linked by bonds, on the other hand, if $r = 0$ all nodes are isolated, for intermediate values of r there will be some sites connected by bonds, while others will be isolated.

If we describe the evolution of fraction of sites (or bonds) belonging to the largest cluster m as a function of the occupied sites (or bonds) fraction r, we would obtain something similar to figure 2, in this way, for very small r, $m(r) = 0$, and for very high r, $m(r) = 1$. Consequently, it is observed that there is a critical value of r, defined as percolation threshold r_c, such that if $r > r_c$ there is at least one path of interconnected nodes that spans the entire network, on the contrary, if $r < r_c$ there are groups of nodes interconnected, but that do not extend throughout the network. This change in the geometric characteristics of the lattice is an example of a continuous phase transition.

Percolation is not studied only considering sites or bonds, there is also the case of their combination [12], as well as the study in more complex systems such as networks (see figure 1 (c)), a typical example is in random graphs [13], where starting from a graph of N isolated nodes, connections are added between them, when rN connections have been added, two cases can occur: if $r < 1/2$, the largest cluster C_1 remains small and scales as $\log N$. If $r > 1/2$, there is a component of linear size in N, that is, $C_1 \approx (4r - 2)N$. So at the critical point $r = 1/2$ the fraction of nodes in the largest cluster undergoes a second order phase transition (see figure 2).

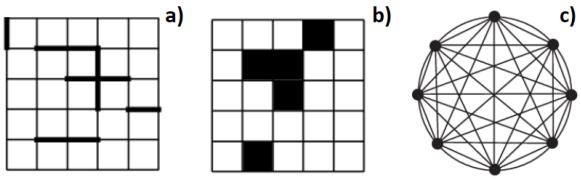

Figure 1: Example of bond percolation (a), site percolation (b) in a square lattice, and percolation in network (random graph) (c). Adapted from https://mathworld.wolfram.com

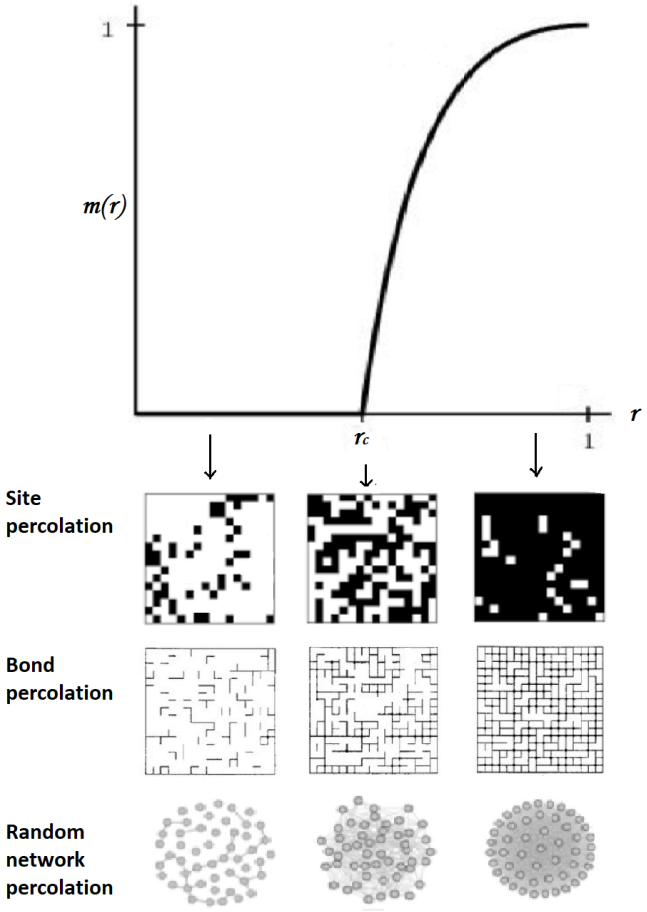

Figure 2: Changes in network connectivity m as a function of sites (or bonds) density r. The percolation threshold r_c determines two phases. In the first phase $r < r_c$ (non-percolating or subcritical phase) the network is manifested by occupied sites (or bonds) that form isolated clusters. The second phase $r > r_c$ (percolation or supercritical phase), increases monotonically with r, the clusters connect when more bonds (or sites) have been added to the network, until a giant component appears. Adapted from: http://www.ams.org/publicoutreach/feature-column/fcarc-percolation, https://faculty.math.illinois.edu/kkirkpat/percolation.html and https://journals.plos.org/plosone/article?id=10.1371/journal.pone.0119979.

2.2.1 Theoretical approach.

Appropriate to the percolation problem, finite-size scaling theory together with the simulation algorithms that we will see later, is one of the most important tools in the study of critical phenomena and phase transitions. The criticality of a percolation system is associated with an order parameter, the way in which this parameter behaves in the vicinity of the critical point is represented by a function that depends on a critical exponent that characterizes universality.

As described in [14], depending on the type of transition finite-size scaling will not work. That is, when the transition is discontinuous (first order), this theory does not work. On the contrary, when the transition is continuous (second order) this theory states that near the percolation threshold r_c the order parameter m of a network composed of N site or bonds, exhibits critical behavior in the limit $N \to \infty$ and obeys the relation:

$$m = N^{-\beta/\nu} F[(r - r_c)N^{1/\nu}], \tag{1}$$

where F is a universal scaling function. β, and ν are the critical exponents and as we have already seen r is the fraction of sites (or bonds) occupied.

Similar laws may be written for others observables, the most common and the one we will use in our work is the susceptibility which quantifies the amplitude of the fluctuations of the percolation strength, defined as $\chi = N\sqrt{\langle m^2 \rangle - \langle m \rangle^2}$, where $\langle m \rangle$ is the first moment or average, and $\langle m^2 \rangle$ is the second moment. χ obeys the relation:

$$\chi = N^{\gamma/\nu} G[(r - r_c)N^{1/\nu}], \tag{2}$$

with G a universal scaling function and γ another critical exponent.

As the order parameter m is directly related to susceptibility χ, it is possible to relate the scaling behavior of m and χ near r_c and derive that $\beta + \gamma = \nu$ [14].

If we consider that at percolation threshold $m_c \equiv m(r_c) \sim N^{-\beta/\nu}$ and $\chi_c \equiv \chi(r_c) \sim N^{\gamma/\nu}$ we can predict these critical exponents by doing a simple linear regression of $\ln(\chi_c)$ versus $\ln(N)$ and $\ln(m_c)$ versus $\ln(N)$.

2.2.2 Percolation algorithm.

The lack of analytical solutions in numerous percolation systems motivated the implementation of different numerical methods for their understanding, algorithms that allow studying ideal systems, where the number of components tends to infinity and multiple configurations can be analyzed under the same conditions to obtain statistics results. The best known are the Leath-Alexandrowicz algorithm [15, 16], the Hoshen-Kopelman algorithm [17] and the Newman-Ziff algorithm [18, 19].

In particular, the Newman-Ziff algorithm [18, 19] based on union-find is widely used for the efficient calculation of percolation or clustering in different configurations based on the number of occupied positions. This algorithm allows to measure the size of the largest cluster based on the number of occupied sites, average size, extension and envelope of the cluster, measurement of the position of the percolation transition, among other useful quantities for the analysis.

This algorithm is based on the idea that if clusters are analyzed in a configuration with N positions occupied, analyzing a configuration with $N+1$ occupied positions can done by simply adding a new occupied position to the previous configuration and study only the next neighbors of this new position.

Instead of creating a completely new state of the lattice for each different value of N that we want to investigate and constructing the groups for that state, the authors propose an algorithm to create a complete set of correct percolation states by adding sites or bonds one by one to the network, starting with an empty network.

The general algorithm is the following:

1. An empty network is initialized.
2. The order in which the sites or bonds will be used is randomly chosen.
3. They start to occupy in that order.
4. Depending on the type of percolation we will have:

   4.1 For bond percolation two situations are distinguished: 1) If the sites connected by the bond belong to different clusters, the clusters are joined into a single one (see bond a of figure 3). 2) If the sites connected by the bond belong to the same cluster, nothing is done (see bond b of figure 3).

   4.2 For site percolation three situations are distinguished: let be j the site to be occupied: 1) If j has two or more occupied neighbors which belong to different clusters these clusters are joined into a single one which also includes the site j. 2) If all the occupied neighbors of j belong to the same cluster, j becomes part of that cluster. 3) If j has no occupied neighbors a new cluster of size 1 is created.
5. Steps 2) and 3) are repeated until all positions have been filled.

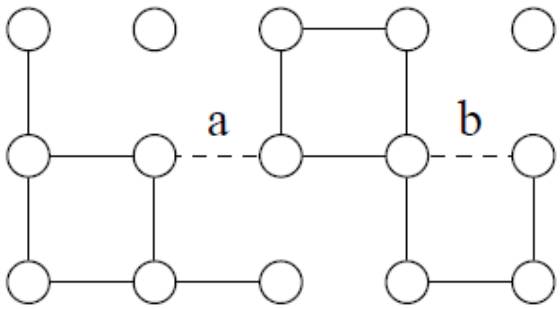

Figure 3: Example of bonds (dotted lines) being added to bond-percolation configurations. Taken from [18].

Clusters are best tracked using a tree-type structure (see Figure 4). Each cluster has a root position that is the root of the corresponding tree. All other elements in the cluster are assigned a pointer that points to the root or to another position in the cluster, so that following successive pointers, the root of the cluster is reached. Pointers are assigned a positive value and roots a negative value, the modulus of which indicates the size of the cluster.

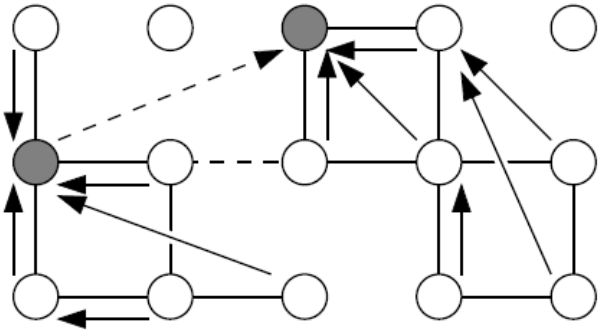

Figure 4: Tree structures example. When adding a link (dotted line in the center) linking sites that belong to different clusters, whose pointers (arrows) lead to different root sites (shaded sites), the two clusters are joined by making one (left) a sub-tree of the other (right). This is accomplished by adding a new pointer from the root of one tree to the root of the other. Taken from [18].

At each step the occupation of an additional site or bond, step 4, implies that clusters may have to be joined. The best known performance algorithm to do so is the "weighted union-find with path compression", as described in [18, 19]. It is based on 2 fundamentals: 1. Weighting: two trees are always joined so that the smaller one is a sub-tree of the larger one. 2. Path compression: The pointers of all nodes along the path traversed to reach the root node are changed to point directly to the root.

The complete algorithm for bond percolation taken from [18] is the next:

1. Initially all sites are clusters in their own right. Each is its own root site, and contains a record of its own size, which is 1.

2. Bonds are occupied in random order on the lattice.

3. Each bond added joins together two sites. We follow pointers from each of these sites separately until we reach the root sites of the clusters to which they belong. Root sites are identified by the fact that they have a negative value associated to the size of the cluster they span. Once the root site of the cluster is reached, the pointer of all the nodes we have traversed is changed so that they point directly to the root. This is the path-compression procedure.

4. If the two root sites are equal then the two sites joined by the bond belong to the same cluster and we do not have to do anything else.

5. If the two root sites are different, we examine their respective size, and change the pointer of the root of the smaller cluster to point to the root of the larger, thereby making the smaller tree a subtree of the larger one. If the two are the same size, we may choose whichever tree we like to be the subtree of the other. We also update the size of the larger cluster by adding the size of the smaller one to it.

6. These steps are repeated until all bonds on the lattice have been occupied.

2.3 Overview and main results in classic percolation.

In the following we proceed to summarize the key results of the classical percolation theory:

1. The higher is r, the larger are the clusters.
2. For a wide range of r values the lattice is populated with numerous tiny clusters, as r approaches a r_c these clusters grow and merge, resulting in a large cluster in r_c.
3. Beyond r_c, there is a finite probability that a node belongs to the largest component.
4. The value of r_c depends on the type of lattice, so it is not universal.
5. The value of r_c changes with the dimension of the lattice.
6. The critical exponents do not depend on the type of lattice or the precise value of r_c, but only on the dimension of the lattice. These exponents are universal.
7. The most used technique in numerical analysis to characterize phase transitions is finite-size scaling theory, since for continuous phase transitions every variable near the critical point scales independent due to the infinite correlation length of the systems at r_c.

2.4 Explosive percolation.

It is known that if the original model is subjected to pre-established conditions, a new percolation model is obtained. This was first considered in reference [1], where researchers explored how a network changes (specifically they compare with the classic Erdos-Rényi model [13] and the bounded-size Bohman and Frieze model [20]) if an element of choice is injected into its formation. To this end they slightly modify the classic bond percolating model in each step several random tries, trials or attempts, and selecting only according to a predetermined rule. The selection rule is based on multiplying the size of the cluster at one end of the bond by the size of the cluster at the other end and choosing the bond that yields the lowest product or sum.

Specifically, to quantify the contribution of a bond to the growth of the largest component, reference [1] uses the sizes of the connecting components. Let e_{12} and e_{34} be two bonds that join nodes 1 with 2 and 3 with 4 respectively (the numbering is arbitrary), and n_1, n_2, n_3 and n_4 are the sizes of the components to which the four nodes belong. The process, known as Achlioptas process or Achlioptas algorithm (see Figure 5) consists in choosing the node that minimizes the product of the sizes of the components, if $n_1 n_2 < n_3 n_4$, we add e_{12} and discard e_{34} (e_{34} may be re-elected in the future). Instead of using this so-called product rule, the sum can also be used, in this case if $n_1 + n_2 < n_3 + n_4$, we add e_{12} and discard e_{34} (see figure 5).

This forced choice (product or sum rule) introduces a bias in the network, an intervention that alters its typical behavior. What happens is that the fluctuations in the average size of the components decrease progressively, homogenizing the size of all of them, but as the bonds are added as a fraction of the total number of nodes, there is a critical value for which a group of connected components are simultaneously connected that percolate into the network massively (instead of adding little by little around the largest component hindered by the rule).

The authors of [1] not only found that this process delays the transition, that is, the beginning of super connectivity, but that by hindering the growth in this way, a kind of pressure is generated, a very violent transition occurs, reaching a critical moment in which the probability that two points are connected jumps from essentially zero to more than 50 percent instantly. Rather than emerging with a slow and steady march toward ever-increasing connectivity like the well-known classical percolation, the connections emerge globally once and for all throughout the system in an abrupt way (see figure 6), in a kind of explosion, resulting in the term "explosive percolation" is already classified as a first-order (discontinuous) transition.

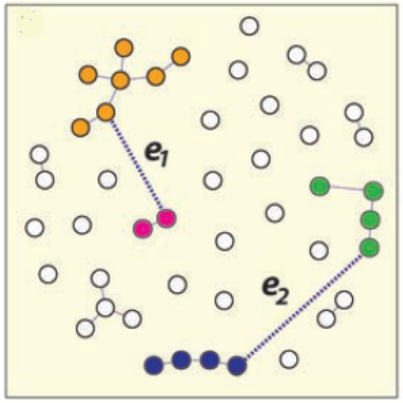

Figure 5: Selection rule example: Because a random system would normally favor the nodes with the most pre-existing connections, instead of letting two random nodes connect or not, two pairs of random nodes e_1 and e_2 are considered and the one generating the smaller cluster is selected. (This method favors the connection between small components or with inversely proportional sizes, preventing large components from joining each other). In this example we have e_1 with $2 \times 7 = 14$ and $2 + 7 = 9$, and e_2 with $4 \times 4 = 16$ and $4 + 4 = 8$, following the product rule, we would choose e_1 and discard e_2, while if we consider the sum rule we would choose e_2 and discard e_1. Taken from [1].

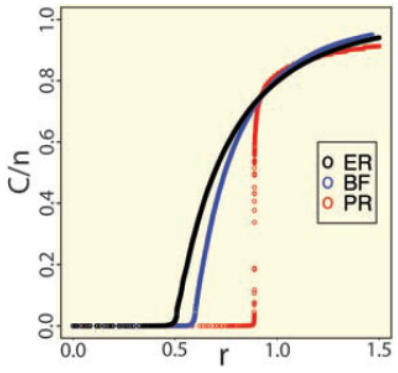

Figure 6: Typical evolution of fraction of nodes belonging to the largest cluster C/N as a function of the occupied nodes fraction r, for Erdos-Renyi (ER) model, Bohman-Frieze (BF) bounded size rule and the Product Rule (PR) process, for n=512.000. Take from [1].

.

Additionally, the authors note that this rule, either the product rule or the sum rule, can be used to accelerate percolating, by selecting the edge that maximizes the product or the sum of the size of the components, but the percolation transition then remains continuous.

2.4.1 Explosive percolation transition.

The idea of introducing a selection rule to the already known classical percolation caused many important additional effects, having greater interest the characterization of its phase transition. Soon after the publication of [1], some studies appear that reveal results similar to those presented by them, however, other investigations showed conclusive evidence that the model introduced there presents a continuous phase transition but with a different kind of universality.

All this debate about the type of phase transition of explosive percolation (see [5, 6, 7] for an explanation of all the studies and results obtained, and [5] for a chronological table of all the results of the literature for the values of r_c and critical exponents is presented) brought with it a series of studies proposing variants of the Achlioptas processes, a combination of different scale relationships at the critical point, extension to other networks, etc. Thus, revealing that there are models of explosive percolation with alternative mechanisms that present discontinuous phase transitions (it is recommended to consult table 2 of [5]), as well as models of explosive percolation that are continuous at the thermodynamic limit but exhibit substantial jumps in the order parameter for any finite system, models that exhibit a single genuine jump in the order parameter long before the end of the process or at the end of the process, as well as non-convergent models that exhibit a ladder with discontinuous steps (see section II D in [6] for more detail in explosive percolation classes).

2.4.2 Directions on the topic of explosive percolation.

The large amount of work that has been done in the area since 2009 has left many novel advances, both for the theory of phase transitions and for modeling a wide range of new phenomena in networks. As it provides a means of manipulating the initiation of long-range connectivity through small-scale interactions, it is believed that it can help to create effective intervention strategies to control the behavior of networks. Connectivity is sometimes wanted to be as large as possible, as for example in operating systems such as the Internet, air networks or the stock market, where they are required to be strongly connected to avoid fragmentation of the network due to damage or attacks. The opposite case occurs, for example, in epidemics, where the objective is to inhibit the spread, reduce the scope of connectivity and make the critical probability as high as possible to avoid contact between different populations.

Explosive percolation has motivated several studies [6] such as explosive Ising model and explosive synchronization, explosive percolation in real world systems (for understanding the evolution of modular network and community structure including evolution processes on the human protein homology network, modeling properties of material and disordered media, non-self-averaging and the emergence of molecular life, explosive immunization, information spreading, etc).

3 Our study.

We want to study explosive site percolation with periodic boundary conditions in a regular network. For that we propose a variant of the sum rule of the Achlioptas algorithm. For its optimization we rely on the weighted union-find with path compression described above.

It is known that phase transitions can be classified based on the behavior of the order parameter, therefore, we consider different order parameters proposed in the consulted literature, together with the basic tools known from finite-size scaling theory for this type of study.

It is important to note that there are few works in the literature where site percolation is studied using the sum rule, most of them just mention it and only [21] studies it in detail. The authors studied site percolation on a L x L square lattice with periodic boundary conditions.

The algorithm for sum rule Achlioptas process taken from [21] is the following:

1. Start from an empty lattice and randomly occupy one single site.
2. Next, randomly select a trial unoccupied site, say A.
3. Calculate the size C_A of the resulting cluster to which A belongs.
4. Remove the trial unoccupied site A and randomly select a trial unoccupied site B, different from A.
5. Calculate the size C_B of the resulting cluster to which B belongs.
6. In case $C_A < C_B$, site A is permanently occupied and site B is discarded. In case $C_B < C_A$, site B is permanently occupied and site A is discarded. In case $C_A = C_B$, we randomly select and permanently occupy either A or B discarding the other. Each time, the number of occupied sites is incremented by one.
7. Repeat steps (2)–(6) until the entire lattice is covered. For each "time step" t , we monitor the size of the largest cluster C_1.

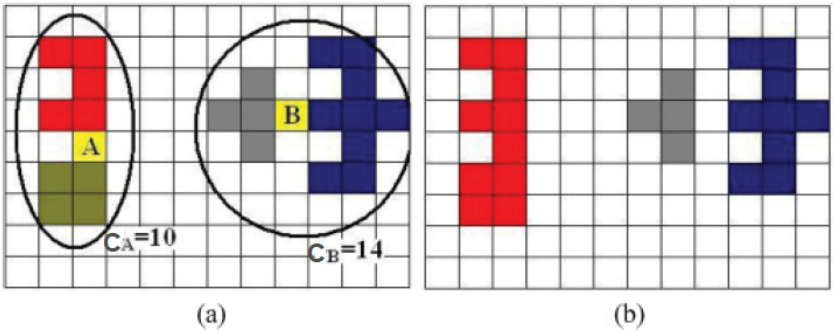

Figure 7: Example of the Achlioptas process according to the sum ruler for site percolation. Unoccupied sites are represented with white cells, colored ones correspond to occupied sites. Color groups (red, green, gray, and blue) indicate different clusters.(a) Randomly select two tries unoccupied sites (A and B, in yellow) one at a time. Evaluate the size of the clusters that are formed and contain sites A and B, C_A and C_B, respectively. (b) According to the rule, site A that leads to the smallest group is kept and B is discarded. Taken from [21].

We follow the same algorithm described with a variant in the rule, we call it *global sum rule*. The principle is: choose the trial site such that the size of the global largest cluster present in the system is the smallest possible (not necessarily containing the added site). In case there are several that would lead to a largest cluster with the same minimal size, then we select the first one. Note that since the selection of the nodes is random, selecting the first try among those that lead to the minimum largest cluster does not introduces any bias (see figure 8 as example).

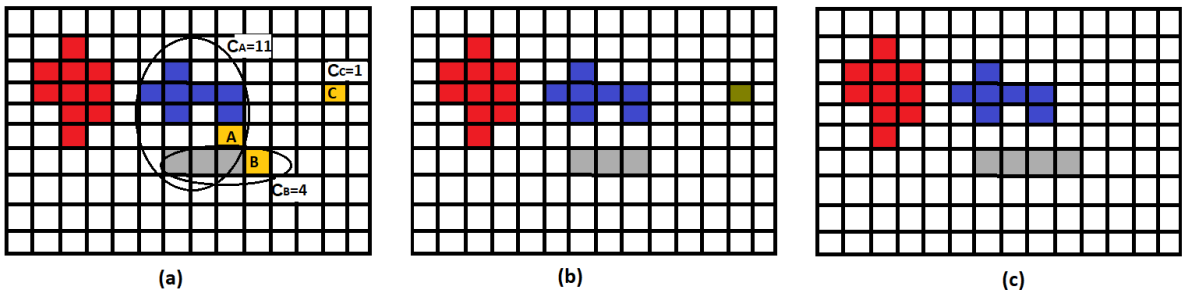

Figure 8: To compare with the ordinary sum rule, consider a case in which there is a cluster of 10 nodes another of 7 and another of 3. (a) Assume there are three tries: A: Adding a node which joins the two smaller clusters which would generate a cluster of 7+3+1=11 nodes. B: Adding a node next to cluster 3, which would generate a cluster of size 4. C: Adding a node which has no occupied neighbors, thus the result would be generating a new cluster of size 1. Try A generates a maximum cluster of 11 nodes which is larger than the result of tries B or C thus this try is disregarded both by the ordinary sum rule and by the global sum rule. (b) Applying ordinary sum rule, try C has to be selected.(c) Applying the global sum rule, since the outcome of try B and try C is that the largest cluster has the same size 10, both tries can be chosen. We choose B because was the first to try among all those that fulfill the condition of generating the minimum largest cluster.

3.1 General system behavior.

Using this algorithm, we start from a regular network with $N = L^d$ sites, where L is the lattice size, and d is the lattice dimension. We define r as control parameter, this is, the fraction of occupied nodes, and $m = C_1/N$ as our order parameter, which represents the fraction of nodes belonging to the largest cluster size C_1.

First we explore the behavior of the system, we evaluate it for several lattice dimensions, and lattice sizes, several number of tries of the global sum rule and several number of realizations.

3.1.1 Lattice dimension.

We fix the lattice size and the number of tries according to the global sum rule and we present results for different spatial dimension (see figure 10). As expected, looking at the order parameter m, we obtain a behavior similar to what is known as explosive percolation, there is a point (critical threshold) at which the behavior of the graph changes. For the sake of clarity we define two zones (see figure 9 as example). We will call zone A the zone where the transition begins, where violent fusion occurs and the order parameter starts to grow very fast, and zone B where the order parameter takes a large value which grows almost linearly with r, where all the trajectories converge, the stable zone. We see that as the dimension increases, the curve of the order parameter shifts to the left, that is, the transition occurs earlier, it is also clear that zone B becomes larger as the dimension of the network increases, which is logical since the greater the connectivity, the faster the percolation threshold is reached.

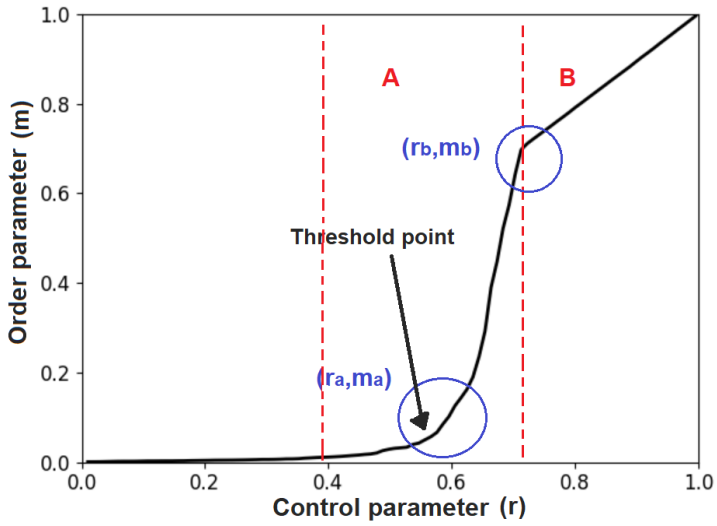

Figure 9: For a better description of the graphic behavior, in what follows we refer to zone A and zone B to those indicated in the figure, in the same way, we define the coordinate axes (r_a, m_a) and (r_b, m_b).

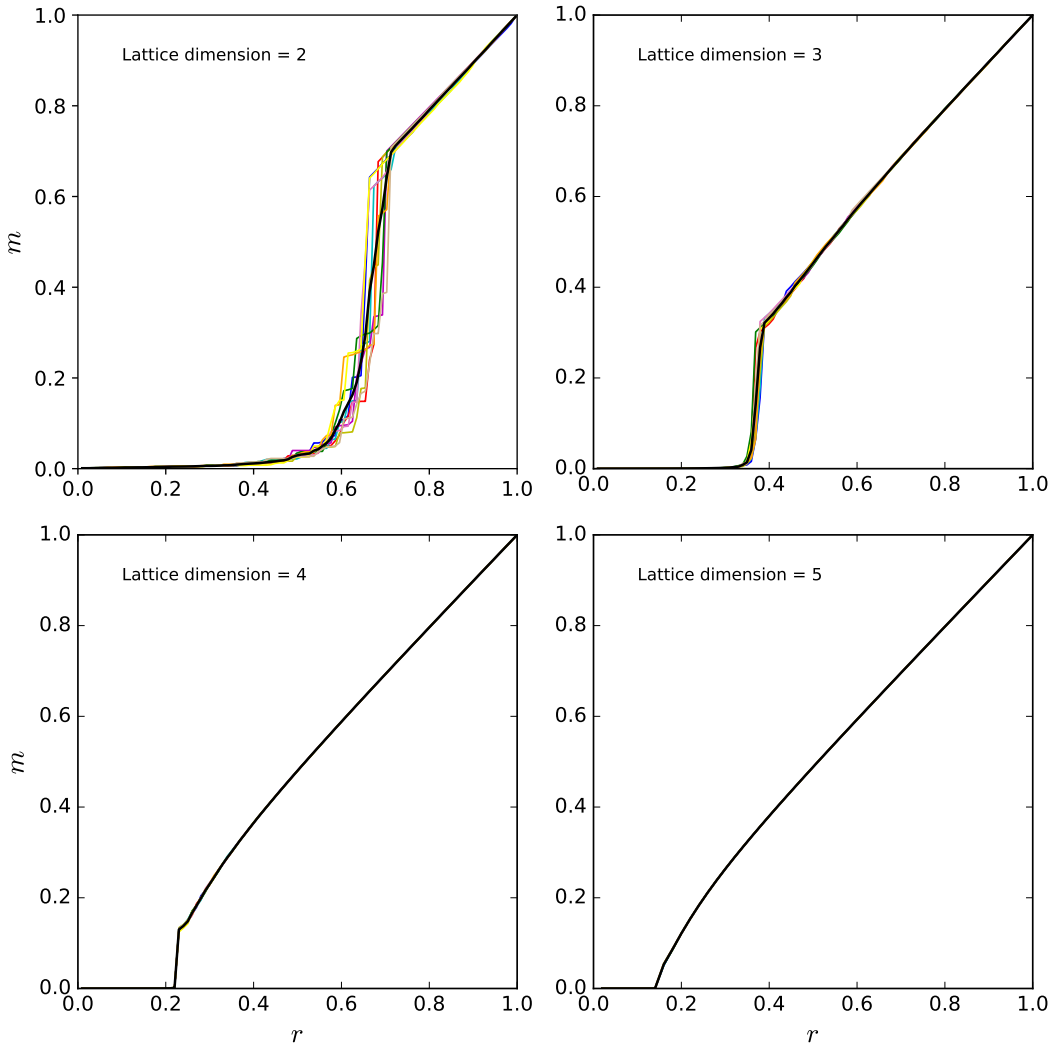

Figure 10: Evolution of fraction of nodes belonging to the largest cluster m as a function of the occupied nodes fraction r for networks of size L=64, and different dimensions. The number of tries according to the global sum rule is 2 in all cases. The black line is the average over 10 different system realizations (colors lines).

3.1.2 Effect of the number of tries in the global sum rule.

Keeping the lattice size and dimension fixed, we observe the behavior of the system when changing the number of tries, for 1 try, of course, we obtain classic percolation, from 2 onward, the behavior described as explosive percolation appears. We see that the greater the number of tries, the curve shifts to the right (larger r values), indicating increasingly delayed transitions. This is logical since as more tries are explored, choosing the one that gives the smallest maximum cluster, makes it more difficult for the maximum cluster to grow. It is important to note that the greater the number of tries, the curves gradually become steeper, m jumps from 0 to 1 within a short interval of r, zone A dominates (see figure 11).

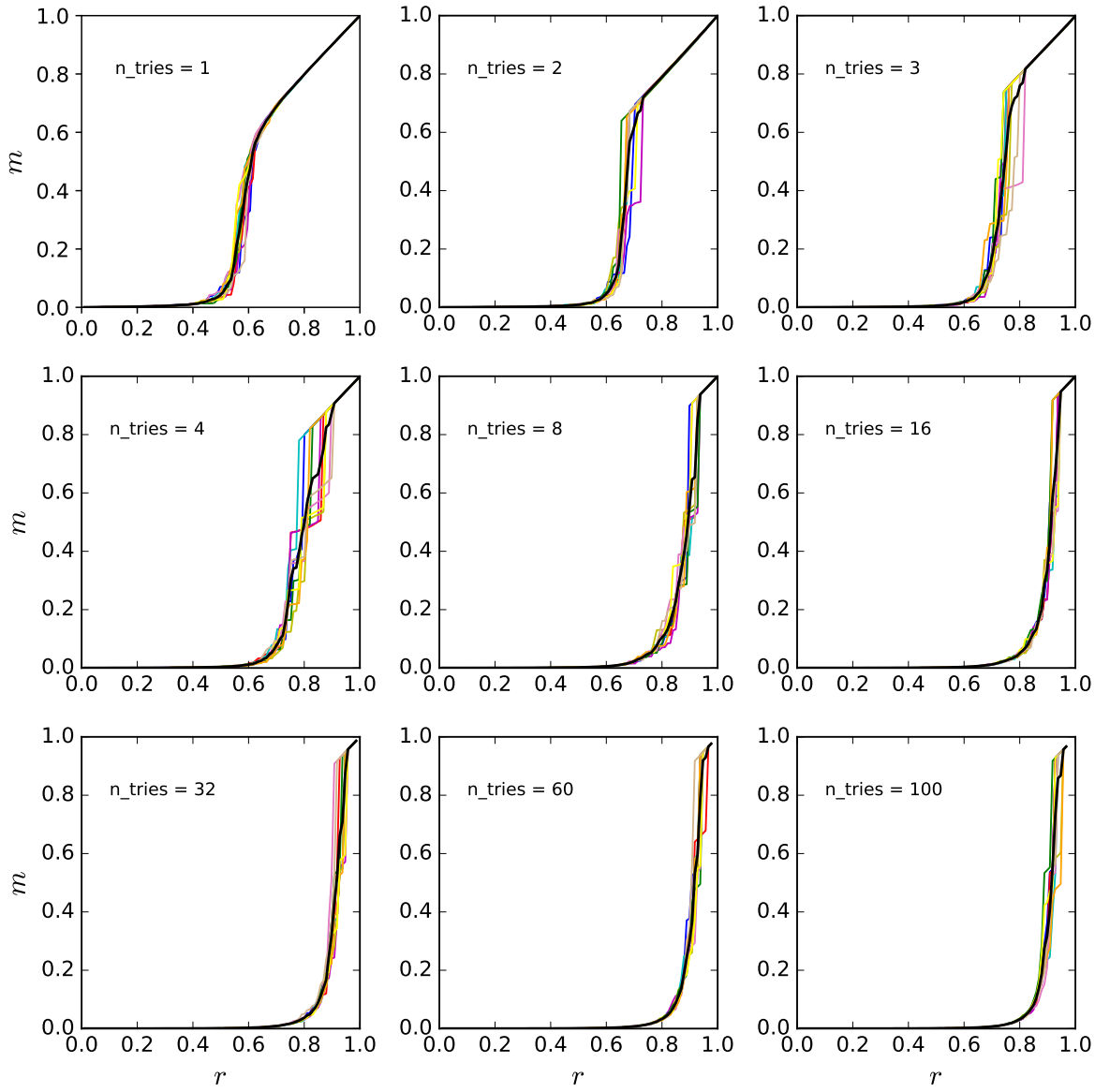

Figure 11: Evolution of fraction of nodes belonging to the largest cluster m as a function of the occupied nodes fraction r for a network of size L= 64, and dimension d= 2, for different values of the number of tries according to the global sum rule. The black line in the results is the average over 10 different system realizations (colors lines).

3.1.3 Lattice size.

To study the behavior when varying the lattice size, we fix the dimension and the number of tries according to the global sum rule, we observe that when the lattice size increases, the curve shifts a little to the right, showing a transition each time more abrupt. We also observe that, similar to the previous cases, as we approach zone B from below, numerous small groups merge, behavior that becomes less visible as the lattice size increases (see figure 12).

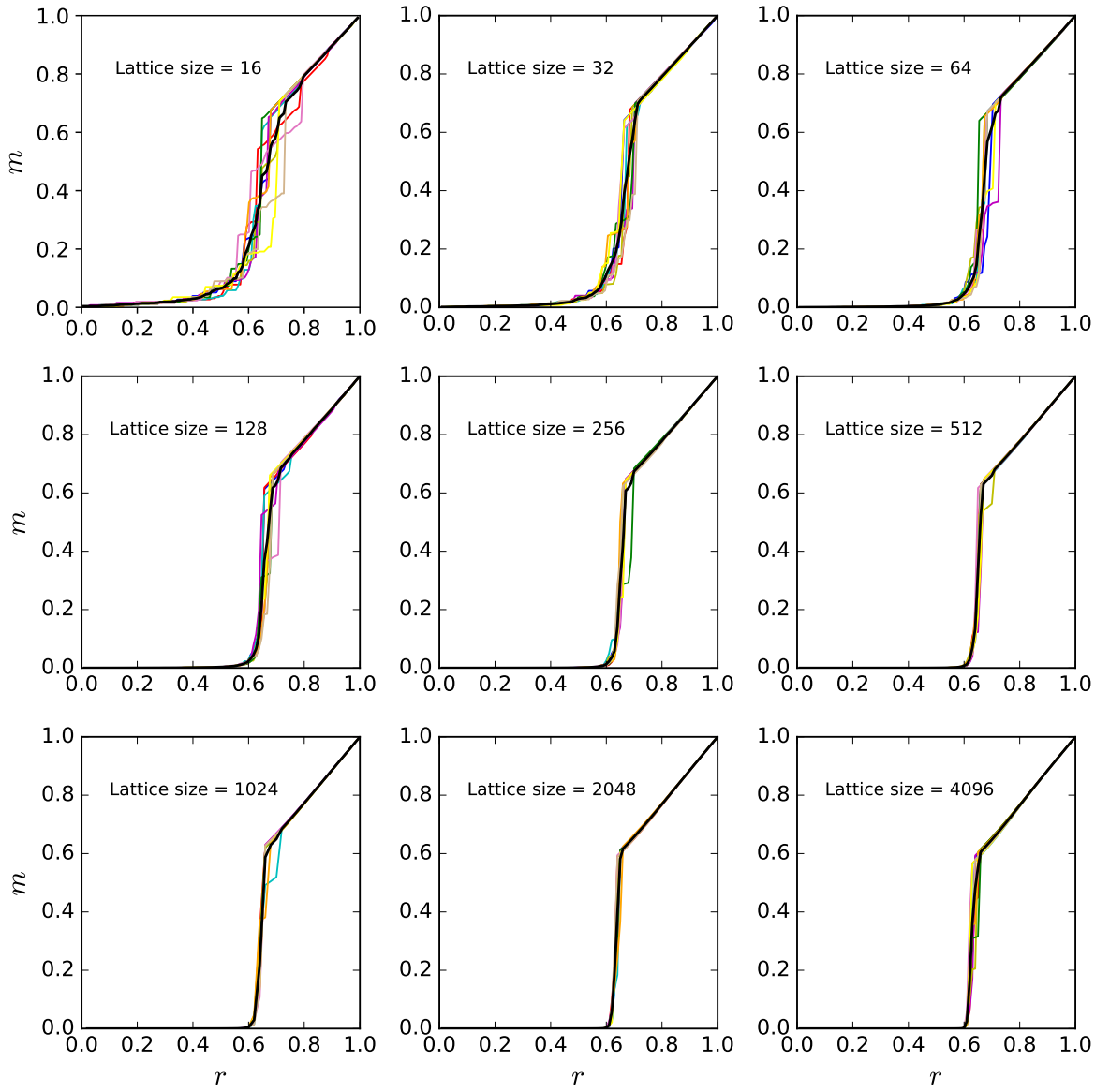

Figure 12: Behaviour of fraction of nodes belonging to the largest cluster m as a function of the occupied nodes fraction r for networks of different sizes, and dimension d=2. The number of tries according to the global sum rule is 2 in all cases. The black line in the results is the average over 10 different number of realizations (colors lines).

3.1.4 Number of realizations.

Finally, we evaluate the statistics over a different number of realizations, we calculate the average and the variance, and we can see how it is expected that the behaviour is the same in all cases, the greater the number of realizations more cleaner are the curves (more noticeable for the variance).

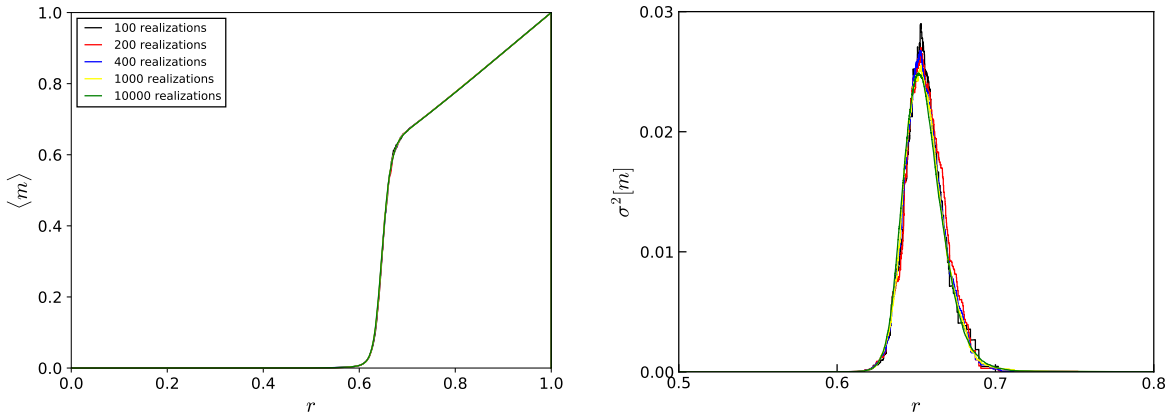

Figure 13: Average and variance of fraction of nodes belonging to the largest cluster as a function of the occupied nodes fraction, for a network of dimension d=2 and size L=512. The number of tries according to the global sum rule is 2 in all cases. The results are averages over different number of realizations.

3.2 Detailed study of 2D lattices.

As we verified in the previous study, obviously, if we repeat the simulation with another set of random numbers, we find a percolation threshold a little different, but as the lattice size increases, the fluctuations decrease until in an infinite lattice all the trials would give exactly the same value of r_c, therefore to obtain better statistics we will work on 10.000 realizations and evaluate lattice sizes of L= 256, 512, 1024 and 2048, numbers that we consider large enough to be able to do an analysis.

In this section we will proceed to study in detail the simplest case, a 2D lattice. Then focusing on the case of 2 tries according to the global sum rule.

3.2.1 Analysis based on largest cluster size.

For this analysis we continue to consider the typical case where m is the order parameter and indicates the fraction of nodes belonging to the largest cluster C_1, and r (fraction of occupied nodes) as the control parameter. We first proceed to evaluate the basic statistical quantities:

$$\text{First moment or Average} \qquad \langle m \rangle = \frac{1}{M} \sum_{i=1}^{M} \left(\frac{C_{1,i}}{N} \right) \tag{3}$$

$$\text{Second moment} \qquad \langle m^2 \rangle = \frac{1}{M} \sum_{i=1}^{M} \left(\frac{C_{1,i}}{N} \right)^2 \tag{4}$$

$$\text{Third moment} \qquad \langle m^3 \rangle = \frac{1}{M} \sum_{i=1}^{M} \left(\frac{C_{1,i}}{N} \right)^3 \tag{5}$$

$$\text{Fourth moment} \qquad \langle m^4 \rangle = \frac{1}{M} \sum_{i=1}^{M} \left(\frac{C_{1,i}}{N} \right)^4 \tag{6}$$

$$\text{Variance} \qquad \sigma = \sqrt{\langle m^2 \rangle - \langle m \rangle^2} \tag{7}$$

$$\text{Susceptibility} \qquad \chi = N\sqrt{\langle m^2 \rangle - \langle m \rangle^2} \tag{8}$$

where M is the number of realizations, and i is the index of the realization..

As we can see in figure 14, we get several interesting things, the greater the number of tries according to the global sum rule, the transition shifts to the right. If zones A and B are evaluated separately, it is curious to note that for 2 tries, for larger moments, zone B predominates and tends to bend upwards, while for 3,4 and 8 tries, zone A predominates and the growth of the moments is practically linear with r. Besides the larger the number of tries, the more separated the trajectories are. On the other hand, it is clear that with 2 tries the transition occurs first for the larger lattice size, while for larger number of tries, the transition occurs first for the smaller lattice.

When studying the variance we see that for 2 tries the curves shift to the left as the lattice increases in size. The opposite to what happens for a higher number of tries, where the curves shift to the right as the size of the network increases. We also see that the larger the lattice the narrower the curve (this is characteristic of a continuous transition). It is evident from the figures that the susceptibility presents the same behaviour.

It is interesting to note that for 2 tries there are two zones where the curves corresponding to different lattice sizes intersect each other, one within zone A and the other at the separation between zones A and B, as exemplified in the figure 9. We will call these 2 crossing points r_a, m_a and r_b, m_b respectively. For higher tries (3, 4 and 8) only the second crossing point r_b, m_b is observed. For more detail see figure 15 and table 1, where it is clearly observed the crossing points for the case of 2 tries. For the case of 3 tries only one crossing point remains (the lower) and for 4 and 8 tries there are no crossing point.

L_1/L_2	**256**	**512**	**1024**	**2048**
256		0.7072, 0.6702	0.6963, 0.6577	0.6912, 0.6469
512	0.6243, 0.0467		0.6883, 0.6484	0.6829, 0.6376
1024	0.6189, 0.0329	0.6149, 0.0201		0.6751, 0.6286
2048	0.6141, 0.0253	0.6113, 0.0154	0.6085, 0.0099	

Table 1: Crossing points r_a, m_a (lower diagonal) and r_b, m_b (upper diagonal) for 2 tries and several lattice sizes.

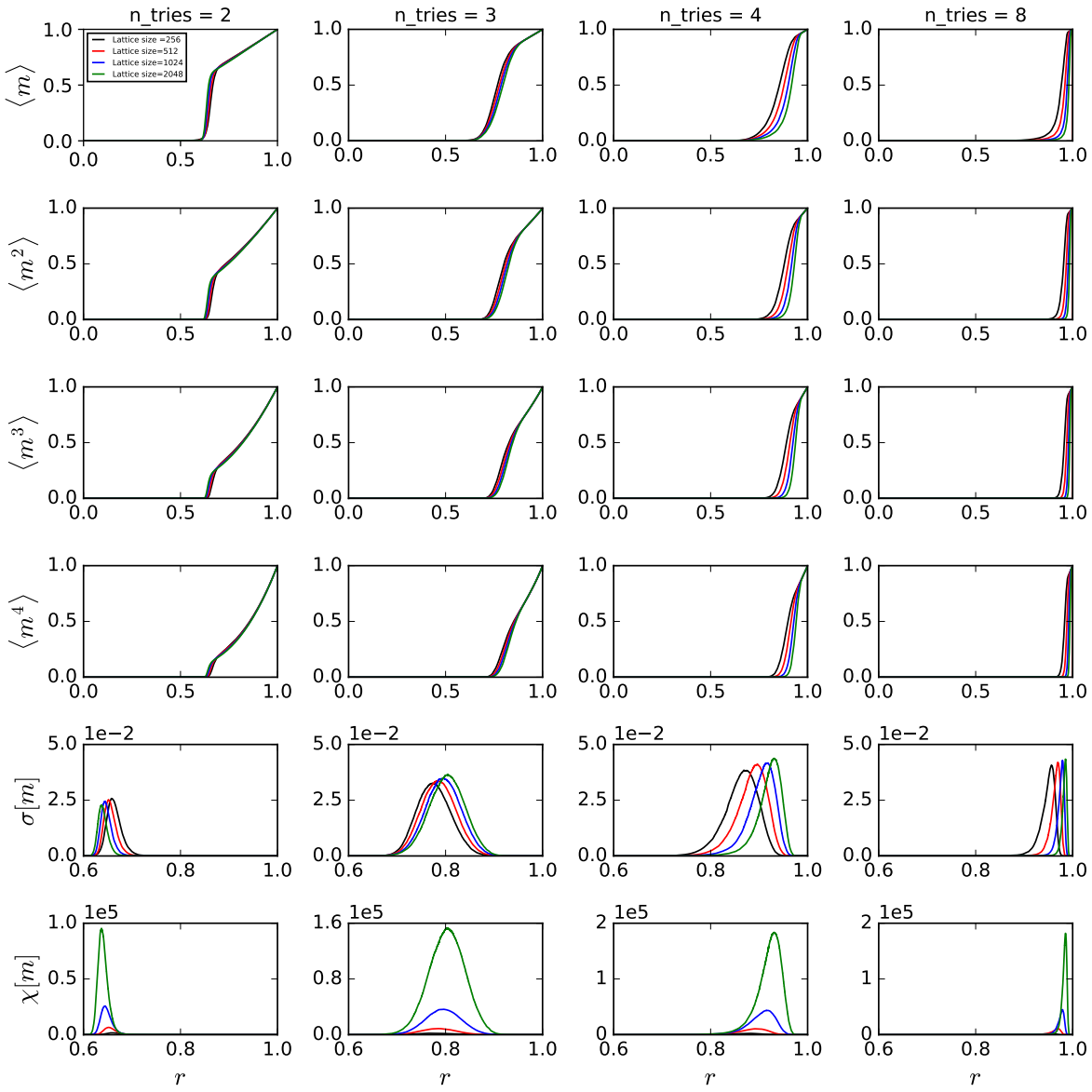

Figure 14: Moments, variance and susceptibility of the fraction of nodes belonging to the largest cluster as a function of the fraction of occupied nodes, for lattices of dimension d=2, and several sizes and for several values of the number of tries according to the global sum rule. The results are averages over 10.000 different system realizations. The black line corresponds to $L = 256$, red to $L = 512$, blue to $L = 1024$ and green to $L = 2048$.

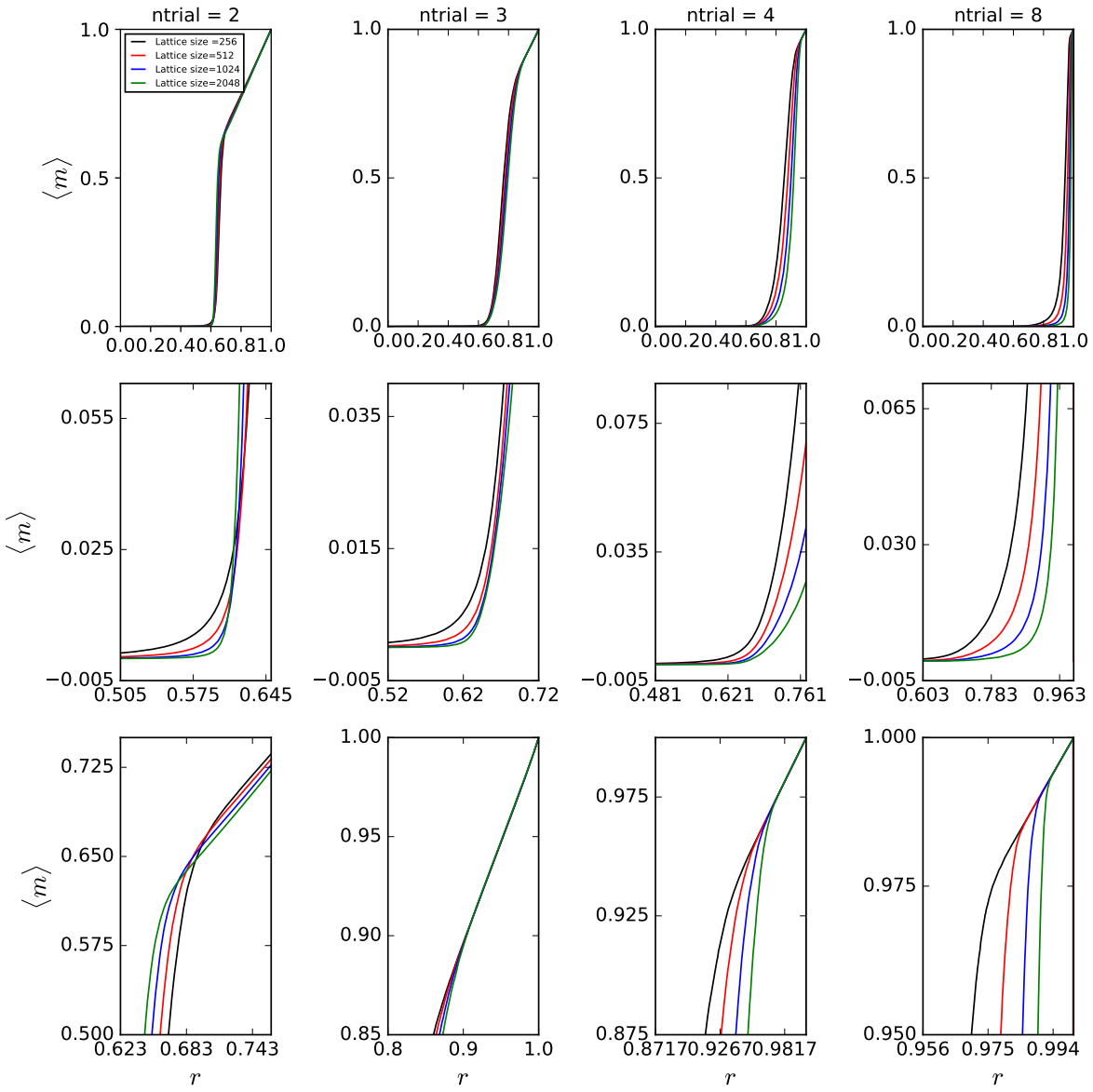

Figure 15: $\langle m \rangle$ vs. r (top panel). Zoom of the first crossover zone (middle panel). Zoom of the second crossover zone (bottom panel).

Then, to estimate the value of r_c when $N \to \infty$ we proceed to evaluate the maximum of the susceptibility and plot this as a function of $\ln(N)$ (see figure 16 and table 2). As we see in figure 14 r_c increases with the number of tries.

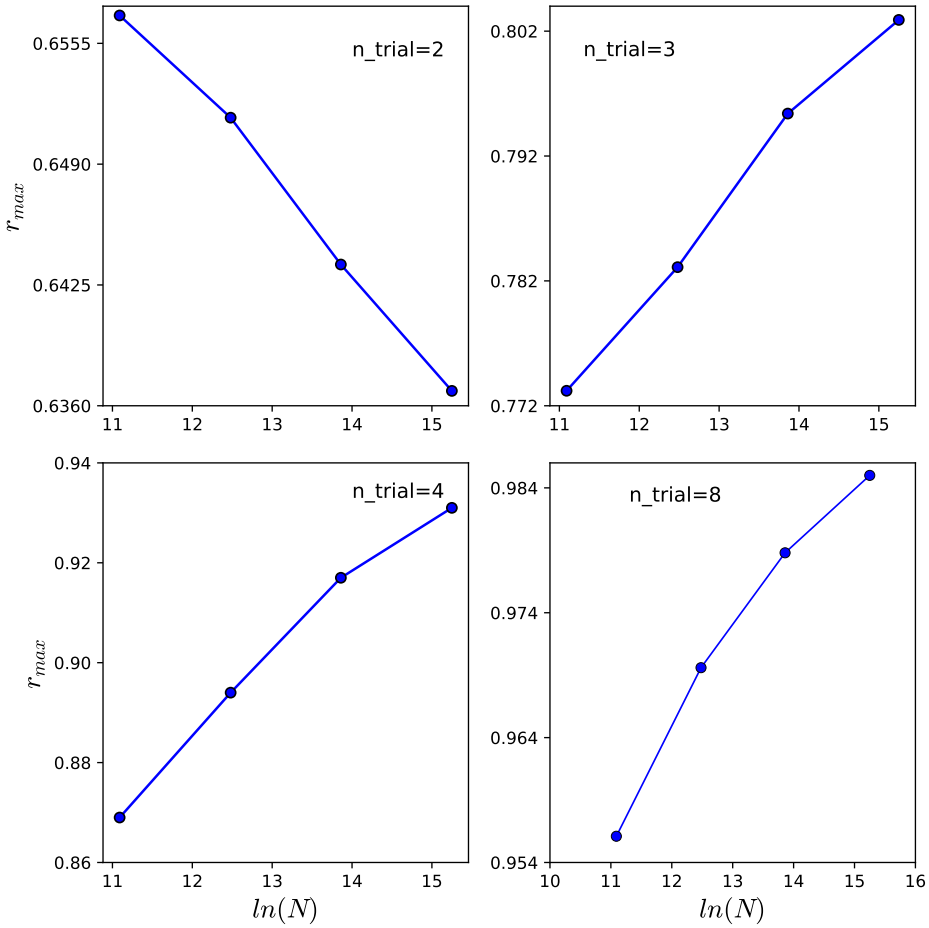

Figure 16: Maximum of the susceptibility χ of the order parameter m as function of $ln(N)$.

Susceptibility maximum	
ntries	r_{max}
2	0.636
3	0.803
4	0.933
8	0.985

Table 2: Values of r_c when $N \to \infty$ estimated from the maximum of the susceptibility for different number of tries.

We now focus on the value of the suceptibility at the maximum for 2 tries. According to the finite-size scaling theory and equation (2), we perform a study of criticality. Using linear regression we calculate the value of the critical exponents γ/ν (see figure 17). Due to the behavior of the order parameter m (it has 2 critical thresholds) it is difficult to apply the scaling relation 1, but following the relation $\beta/\nu + \gamma/\nu = 1$ and the results obtained for $\gamma/\nu = 0.939 \pm 0.043$, we can deduce that $\beta/\nu \simeq 0.061 \pm 0.043$, practically trivial values $\gamma/\nu = 1$, $\beta/\nu = 0$ so it is difficult to characterize the transition.

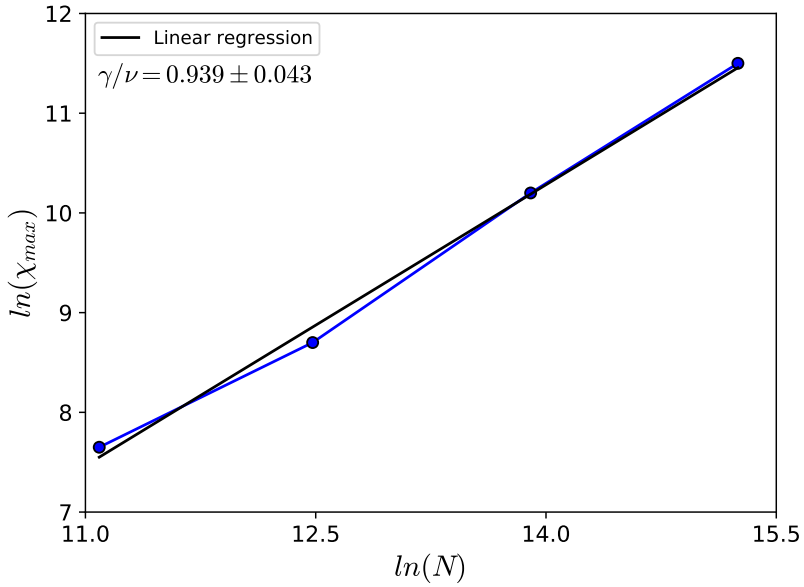

Figure 17: Logarithm of the maximum of the susceptibility $ln(\chi_{max})$ of the order parameter m vs. $ln(N)$ (blue line). The black line corresponds to a linear regression $y = (0.939 \pm 0.043)x - (2.86 \pm 0.57)$. We have considered the global sum rule with 2 tries.

To continue in the same line of analysis we calculate the Binder cumulant [22] :

$$U_4 = 1 - \frac{\langle m^4 \rangle}{3\langle m^2 \rangle^2}. \tag{9}$$

and we evaluate their behavior as a function of r for different values of the system size. It's known that when $N \to \infty$, r_c is the unique point where the different curves cross, as in the critical region $U_4(r, L) = U_4[(r - r_c)L^{1/\nu}]$.

As we can see in the figure 18 the behavior in general is very peculiar, it is striking that for all the number of tries considered we find two crossing points, which we proceed to evaluate in detail (see figure tables 3 and 4). The values shown in the tables are not precise, since despite having smoothed the curves, they are very dirty and we cannot accurately identify the value of these points for 3,4 and 8 tries. Also we can see that the values of r_b are what more or less resemble those obtained when evaluating the maximums of the susceptibility. With this and the previous results we can say that in this case the usual form of the finite-size scaling theory does not apply.

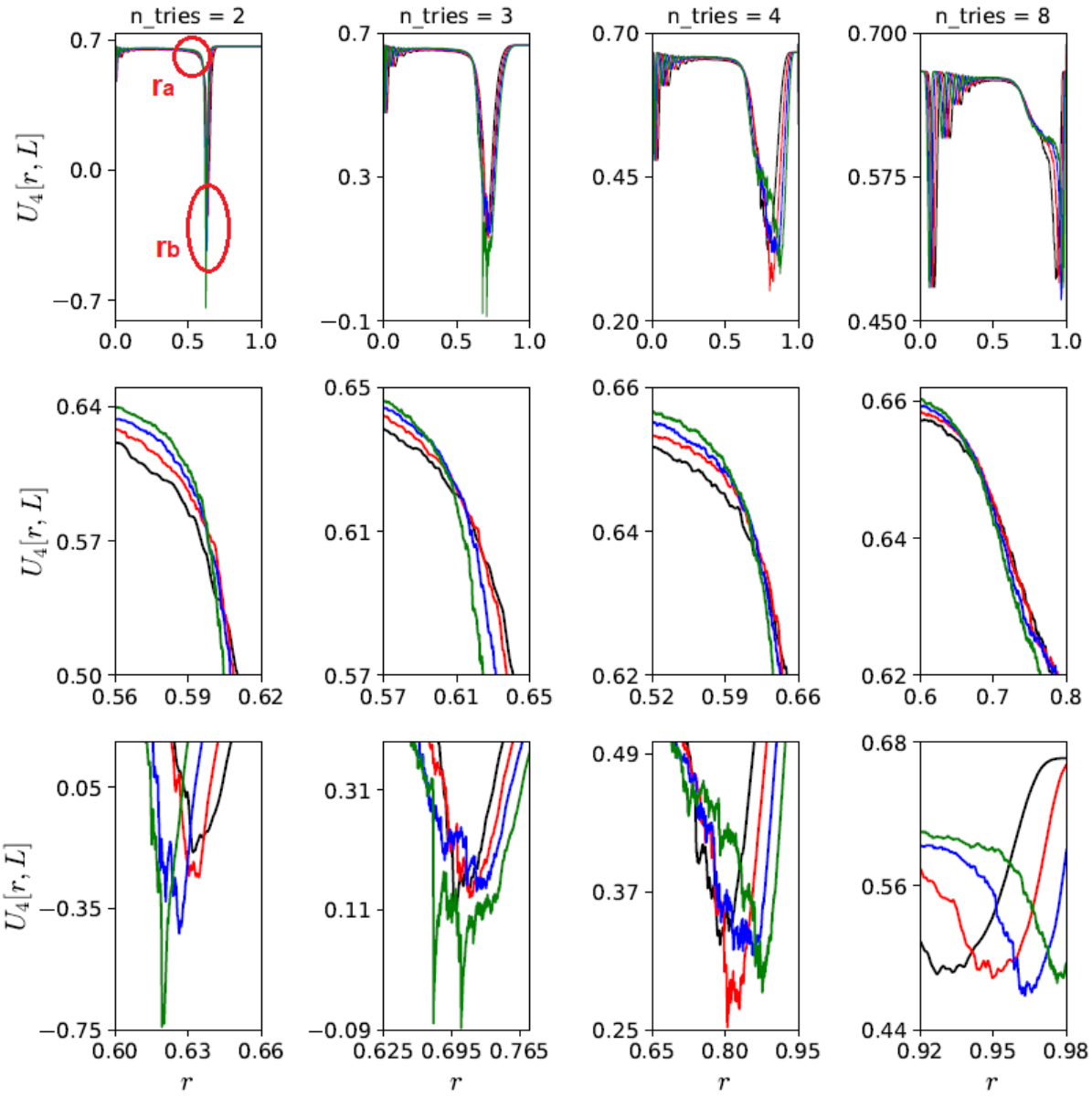

Figure 18: Binder cumulant (top panel) for network of dimension d=2 and sizes L= 256 (black), 512 (red), 1.024 (blue) and 2.048 (green) for different values of the number of tries according to the global sum rule. Zoom of the first crossover zone r_a (middle panel). Zoom of the second crossover zone r_b (bottom panel).

Binder cumulant		
ntries	r_a	r_b
2	0.601 ± 0.007	0.629 ± 0.009
3	0.61 ± 0.01	—
4	0.62 ± 0.02	0.834 ± 0.05
8	0.67 ± 0.04	0.957 ± 0.02

Table 3: Estimated values for r_a and r_b from the Binder cumulant, corresponding to several number of tries according to the global sum rule. Dashes indicate that it was impossible give an estimation for the point.

L_1/L_2	**256**	**512**	**1024**	**2048**
256		0.6363, -0.098	0.6308, -0.080	0.6275, 0.067
512	0.6043, 0.5336		0.6297, -0.207	0.6268, -0.019
1024	0.6043, 0.5316	0.5977, 0.5749		0.6231, -0.274
2048	0.6014, 0,5403	0.5977, 0.5749	0.5749, 0.5749	

Table 4: Crossing points r_a, U_{4a} (lower diagonal) and r_b, U_{4b} (upper diagonal) for lattices of several sizes.

3.2.2 Analysis based on the cluster size distribution.

As the previous results are not clear or conclusive, we proceed to consider other order parameter proposed in [23], the second moment of the cluster size distribution:

$$\langle m_2^2 \rangle = \left\langle \sum_i \frac{s_i^2}{N_c} \right\rangle, \tag{10}$$

where $\langle \cdots \rangle$ denotes average over realizations, the sum runs over all clusters i, s_i is the size of cluster i, and N_c indicates the number of clusters.

When evaluating this new order parameter, we see that initially the curves are separated, and as r increases, they converge. There are also 2 crossing points (see figure 19), which, as in the previous cases, proceed to evaluate in detail (see table 5). In this case we obtain that $r_a = 0.615 \pm 0.020$ and $r_b = 0.666 \pm 0.010$.

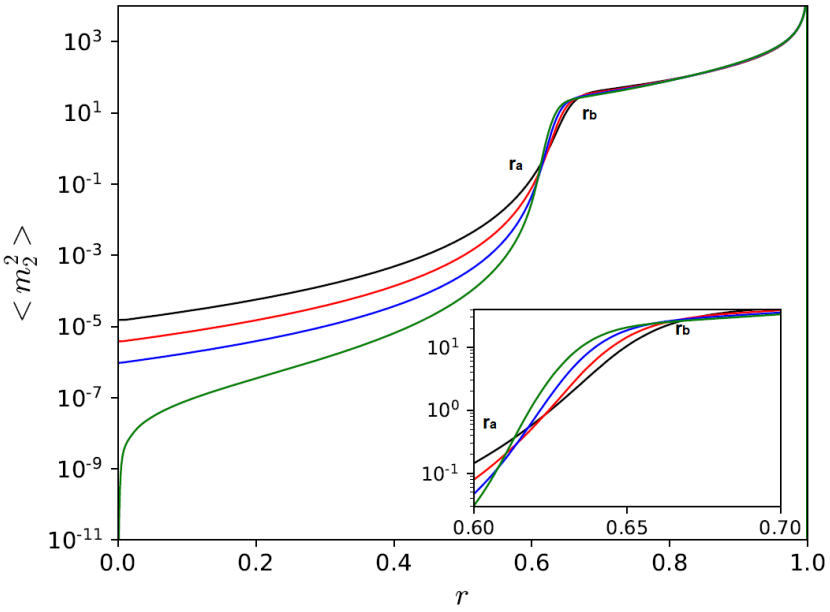

Figure 19: Second moment of cluster size distribution, for network of dimension d=2 and sizes L= 256 (black), 512 (red), 1.024 (blue) and 2.048 (green) for 2 tries according to the global sum rule.

$L_1 L_2$	256	512	1024	2048
256		0.673, 30.805	0.677, 28.282	0.668, 26.536
512	0.623, 0.839		0.667, 27.684	0.663, 25.417
1024	0.617, 0.525	0.614, 0.303		0.658, 24.010
2048	0.613, 0.365	0.610, 0.202	0.608, 0.124	

Table 5: Crossing points $r_a, < m_{2a}^2 >$ (lower diagonal) and $r_b, < m_{2b}^2 >$ (upper diagonal) for lattices of several sizes.

3.2.3 Analysis based on cluster size distribution disregarding the largest cluster.

Motivated by [14], we evaluate how the parameter $\langle m_2^2 \rangle$ studied above changes when the maximum cluster is not considered. For that we define a new order parameter:

$$\langle m_3 \rangle = \left\langle \sum_i{}' \frac{s_i^2}{N_{c-1}} \right\rangle, \tag{11}$$

where $\langle \cdots \rangle$ denotes average over realizations, the sum runs over all clusters i except the largest cluster, and N_{c-1} indicates the number of clusters except the largest cluster.

The figure 20 shows the behavior of the system and its susceptibility. As before, we proceed to evaluate in detail the 2 crossing points (see table 6) and the maximums of the susceptibility in order to obtain the critical threshold. In this case for ntries=2 we find that the value of r_c when $N \to \infty$ is $r_{max} \approx 0.632$. In the same way, we performed the finite-size scaling analysis to

try to calculate the critical exponents (see figure 21), for what we find that $\gamma/\nu = 0.904 \pm 0.031$ and $\beta/\nu \simeq 0.096 \pm 0.031$, similar values found in the analysis presenting in the section 2.2.1.

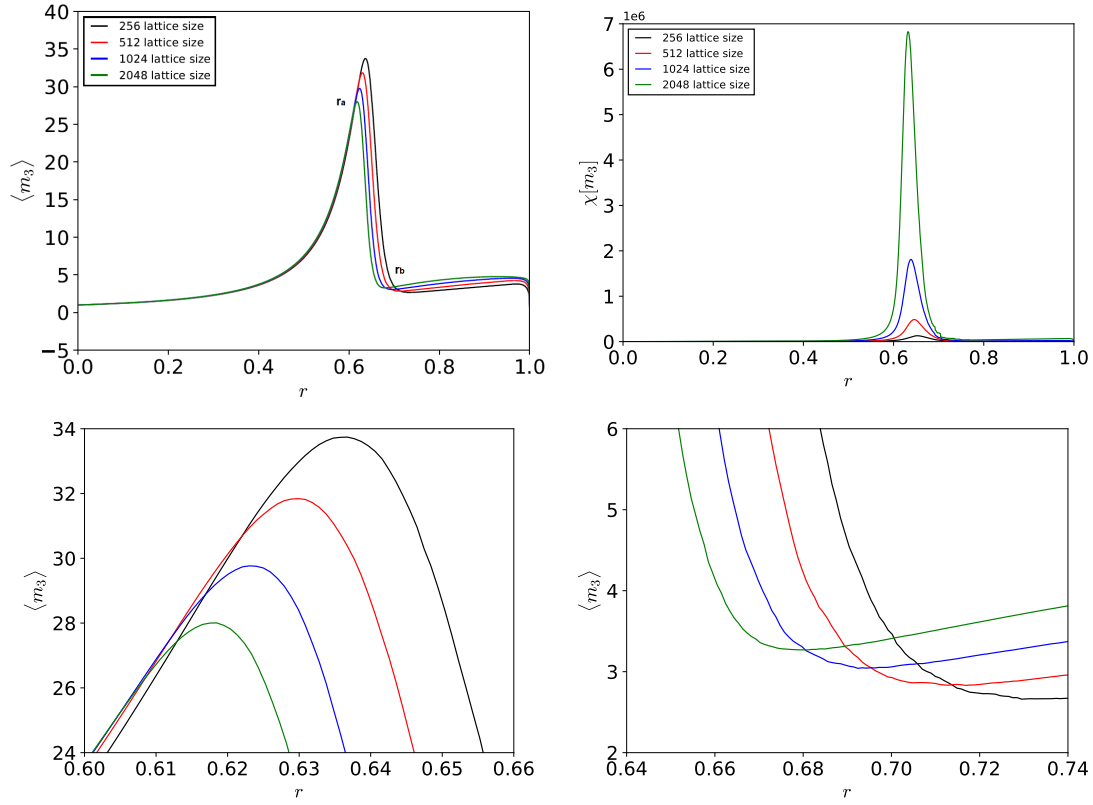

Figure 20: Average and susceptibility disregarding the largest cluster, for lattices of dimension d= 2 and sizes L= 256 (black), 512 (red), 1.024 (blue) and 2.048 (green) using the global sum rule with 2 tries (Top panel). Zoom of the first crossover zone r_a (bottom left panel). Zoom of the second crossover zone r_b (bottom right panel).

$L_1 L_2$	256	512	1024	2048
256		0.713, 2.87	0.706, 3.08	0.700, 3.45
512	0.622, 30.71		0.695, 3.05	0.690, 3.33
1024	0.617, 28.96	0.613, 27.68		0.680, 3.28
2048	0.613, 27.44	0.608, 26.28	0.609, 26.46	

Table 6: Crossing points r_a, m_{3a} (lower diagonal) and r_b, m_{3b} (upper diagonal) for lattices of several sizes.

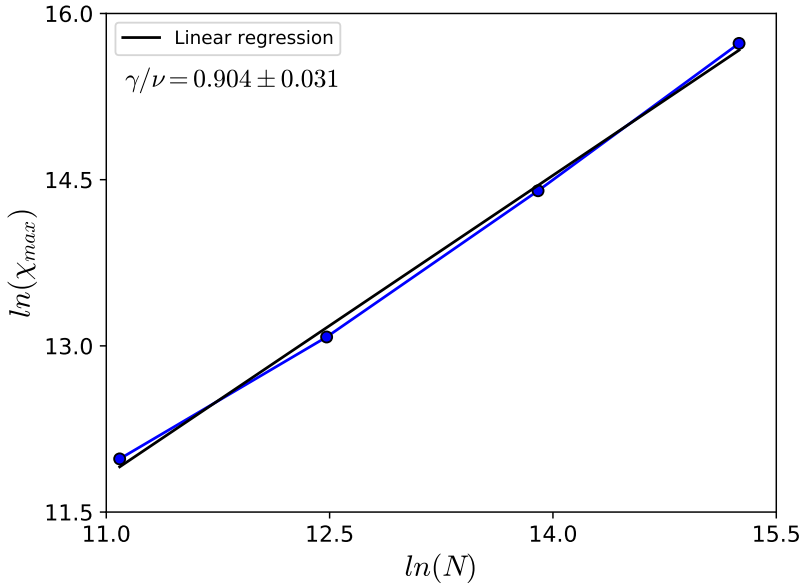

Figure 21: Logarithm of the maximum of the susceptibility $ln(\chi_{max})$ of the order parameter m_3 vs. $ln(N)$ (blue line). The black line corresponds to a linear regression $y = (0.904 \pm 0.031)x + (1.88 \pm 0.41)$. We have considered the global sum rule with 2 tries.

3.2.4 Analysis based on the size ratio of the second largest cluster to the largest cluster.

Finally, we explore the size ratio of the second largest cluster to the largest cluster. As [24] remarks, near the critical point, the size C_2 of the second largest cluster and the size C_1 of the giant cluster, demonstrate critical behavior, which is interesting to study. We define the new order parameter as:

$$\langle m_4 \rangle = \left\langle \frac{C_2}{C_1} \right\rangle . \tag{12}$$

where $\langle \cdots \rangle$ denotes average over realizations.

In this case, as we can see in 22, there is only one region with crossing points (see table 7). For its crossing point, we get the critical threshold 0.623 ± 0.01.

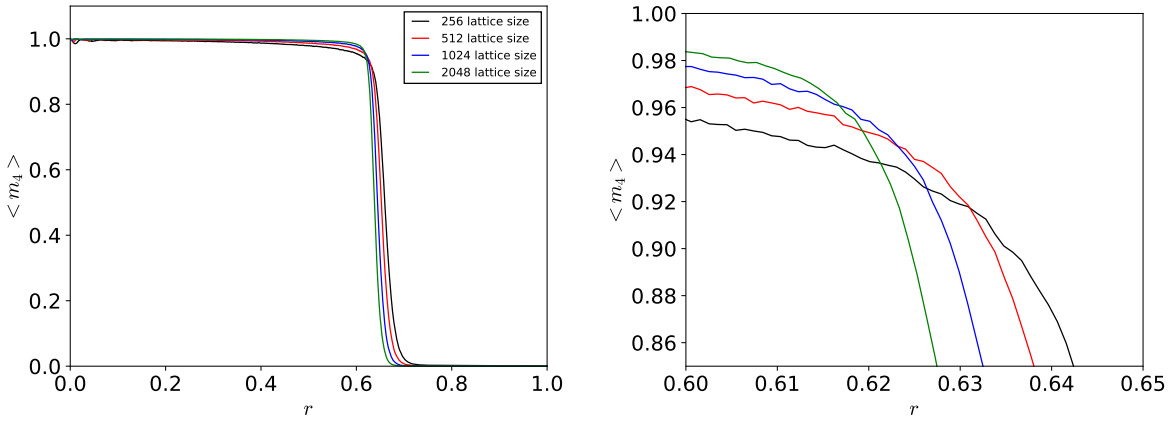

Figure 22: Size ratio of the second largest cluster to the largest cluster, for network of dimension d=2 and sizes L= 256 (black), 512 (red), 1.024 (blue) and 2.048 (green) for 2 tries according to the global sum rule.

L_1/L_2	256	512	1024	2048
256				
512	0.6311, 0.9176			
1024	0.6263, 0.9251	0.6232, 0.9435		
2048	0.6211, 0,9364	0.6192, 0.9506	0.6168, 0.9609	

Table 7: Crossing points r_a, m_4 for lattices of several sizes.

3.2.5 Critical threshold analysis.

In the table 8 we can see the value of the critical threshold found for each parameter that we have considered in this study (for the case of the first order parameter studied, m we only consider the values obtained with 2 tries of the global sum rule). For a better visualization of the data we can see figure 23. In the case of r_a we can observe that $\langle m \rangle$, $\langle m_3 \rangle$ and $\langle m_2^2 \rangle$ tend to the same critical point. $\langle m_4 \rangle$ (although more distant) has a similar behavior, while as expected the Binder cumulant moves further away. According to the results obtained, we see that the value of r_a is within a range of $(0.594 - 0.613)$ that is 0.6035 ± 0.0095. Similar behavior although the curves are more distant from each other is observed for r_b, in this case its value is within a range $(0.620 - 0.717)$ that is 0.669 ± 0.049. On the other hand, the maximums of the susceptibility corresponding to $\langle m \rangle$ and $\langle m_3 \rangle$ indicate values between $(0.632 - 0.636)$, that is 0.634 ± 0.002.

Then to better observe the behavior of the parameters at the crossing points, we proceed to plot them as a function of $ln(N)$ (see figure 24), we see that in general the point r_a decreases for parameters of order $\langle m \rangle$, $\langle m_2^2 \rangle$, $\langle m_3 \rangle$ while it increases for $\langle m_4 \rangle$, With respect to the Binder cumulant it seems to tend to a constant. In r_b the order parameters $\langle m \rangle$ and $\langle m_3 \rangle$ tend to a constant, while for $\langle m_2^2 \rangle$ and the Binder cumulant decreases.

Parameter	r_a	r_{max}	r_b
$\langle m \rangle$	0.615 ± 0.01		0.690 ± 0.02
$\chi[m]$		0.636	
$U_4[m]$	0.601 ± 0.007		0.629 ± 0.009
$\langle m_2^2 \rangle$	0.615 ± 0.02		0.666 ± 0.01
$\langle m_3 \rangle$	0.613 ± 0.01		0.697 ± 0.02
$\chi[m_3]$		0.632	
$\langle m_4 \rangle$	0.623 ± 0.01		

Table 8: Critical threshold for the different parameters studied.

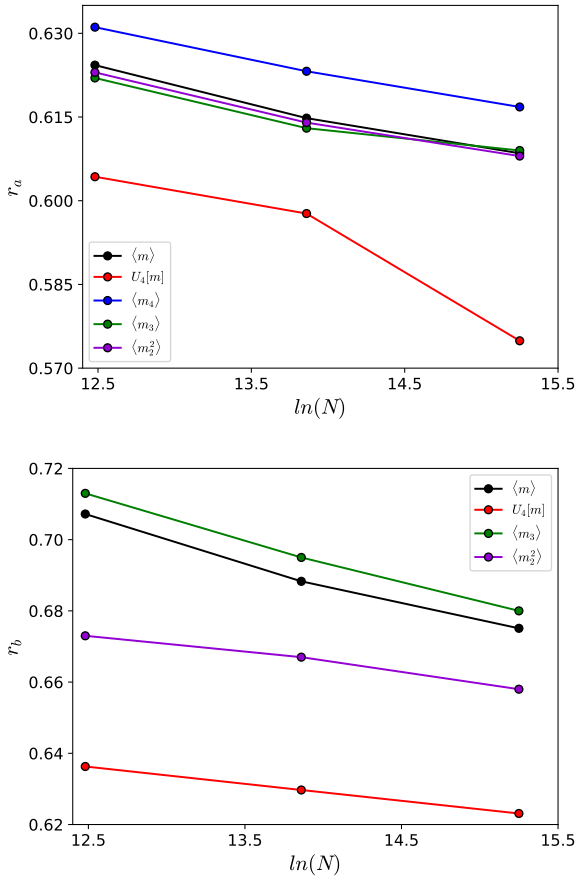

Figure 23: r_a vs lnN (top panel) and r_b vs lnN (bottom panel) for the different parameters studied.

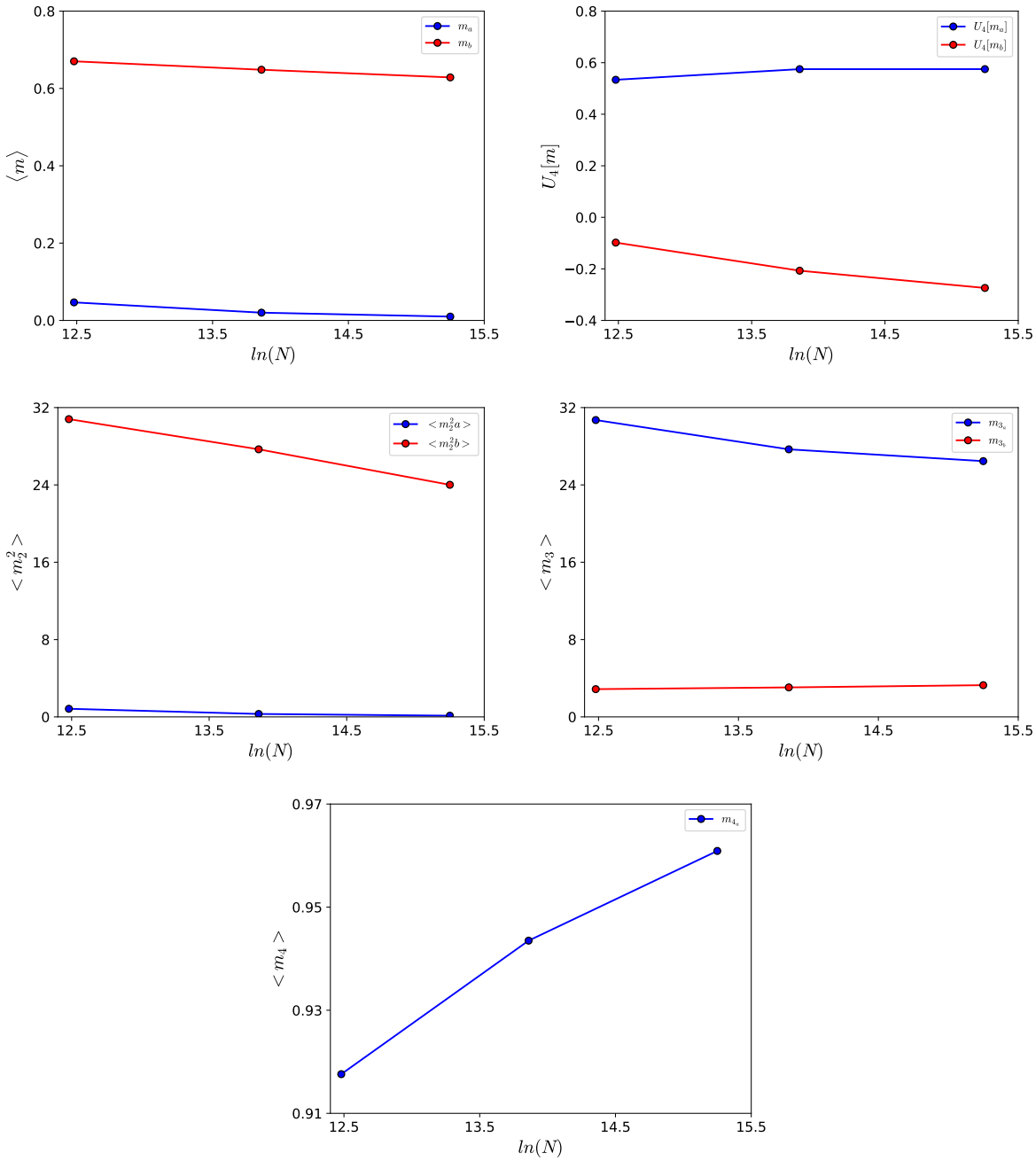

Figure 24: Behavior of the parameters studied as a function of $ln(N)$ at the crossing points.

3.3 Brief general analysis in 3D, 4D and 5D.

As the size of the networks grows, the computational calculation time increases considerably. For this reason for the case of larger dimensions we did not carry out a detailed study like the previous one, but we will show a brief descriptive analysis of the behavior of the system when evaluating the moments, variance and susceptibility, considering $m = C_1/N$ as order parameter. In this case we work with networks of dimension 3,4, and 5; and networks of size L= 8, 16, 32 and 64. For computational reasons for the case of 5D the simulation was not carried out for $L = 64$ but this was not relevant for our analysis.

When evaluating the case for 3D (see figure 25), we observed 2 crossing points for all numbers of tries, as well as a slight shift to the right of the phase transition. If we compare with the behavior in 2 dimensions we see that the zone B is larger for all cases, even as the moments increase, this zone dominates, adopting the form of an exponential. Another difference that is observed is that transitions occur earlier. When analyzing the variance we see that it shifts to the right as the number of tries increases, also that the larger the lattice size it narrows (except for 8 tries).

In the case of 4D (see figure 26), the general behavior is the same, only more pronounced, an aspect to highlight with respect to 2D and 3D is the fact that the variance curves begin to separate.

In 5D (see figure 27) we can see that there is only one crossing point, also when increasing the number of tries and moments, a very slight shift to the right is observed. For the variance in all cases except for 8 tries, the curve is larger the smaller the lattice size.

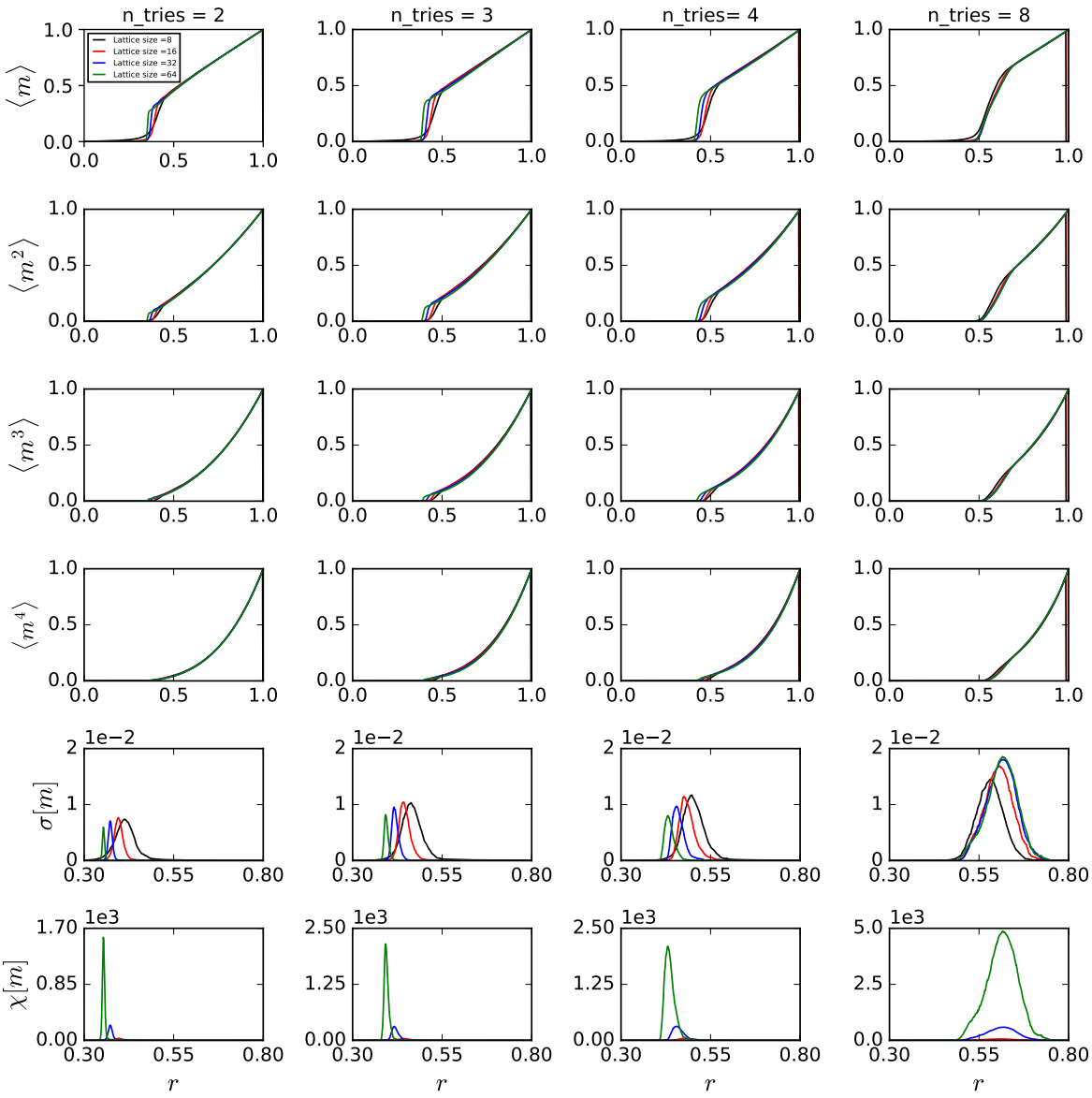

Figure 25: Moments, variance and susceptibility of fraction of nodes belonging to the largest cluster as a function of the occupied nodes fraction, for lattices of dimension d=3, and several sizes and for several values of the number of tries according to the global sum rule. The results are averages over 1.000 different system realizations. The black line corresponds to $L = 8$, red to $L = 16$, blue to $L = 32$ and green to $L = 64$.

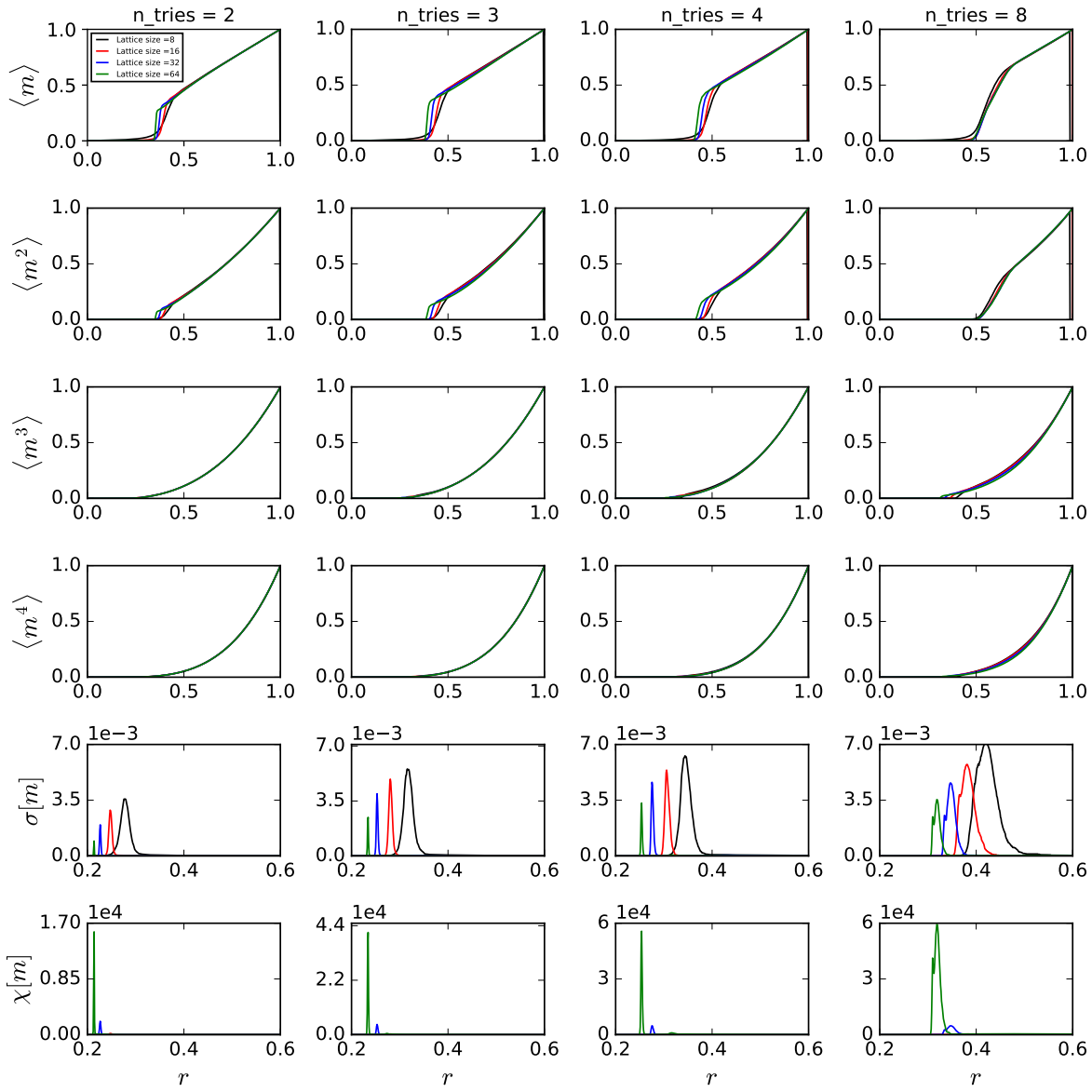

Figure 26: Moments, variance and susceptibility of fraction of nodes belonging to the largest cluster as a function of the occupied nodes fraction, for lattices of dimension d=4, and several sizes and for several values of the number of tries according to the global sum rule. The results are averages over 1.000 different system realizations. The black line corresponds to $L = 8$, red to $L = 16$, blue to $L = 32$ and green to $L = 64$.

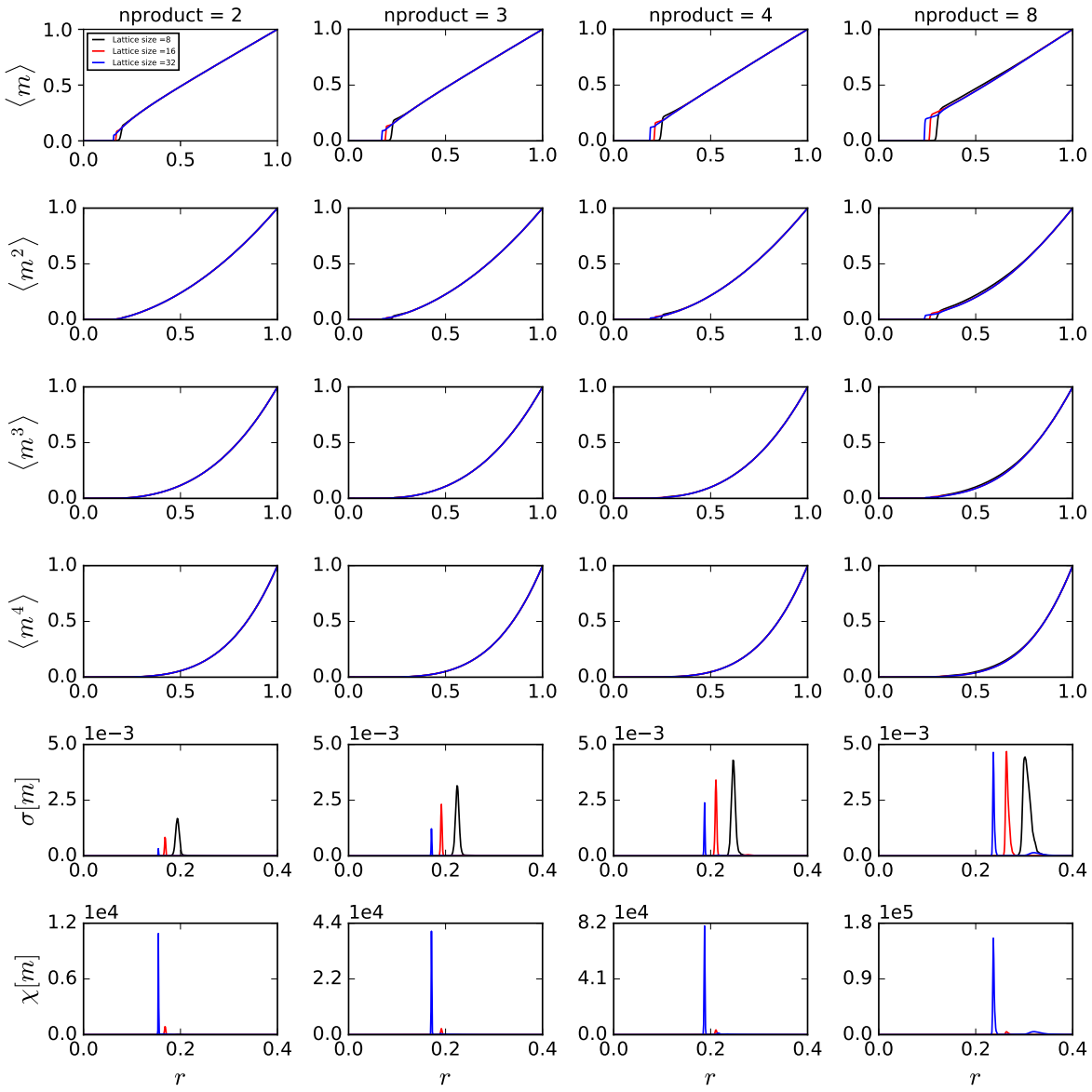

Figure 27: Moments, variance and susceptibility of fraction of nodes belonging to the largest cluster as a function of the occupied nodes fraction, for lattices of dimension d=5, and several sizes and for several values of the number of tries to the global sum rule. The results are averages over 1.000 different system realizations. The black line corresponds to $L = 8$, red to $L = 16$ and blue to $L = 32$.

4 Conclusions

In this work we have proposed a variant to the well known Achlioptas sum algorithm to study explosive site percolation. We have analyzed the behavior of the transition for different network sizes and tries of the global sum rule. We have studied the critical behavior using several order parameters, and we have obtained very similar values of r_c. In the same way we have used finite-size scaling analysis to obtain the values of the critical exponents, and we have obtained results that agree with the majority of those reported in the bibliography (see table 1 of the reference [5]). On the other hand, we have observed that for this system the Binder cumulant is not a suitable order parameter, which probably explains why it has not been used in the studies carried out so far on the subject.

Based on the results obtained, we cannot say with certainty the order of the type of transition, but there are strong indications of being discontinuous. This is also consistent with the majority of published results where the authors define it as a discontinuous transition but with characteristics typically associated to second-order scale behavior, a class of universality different from those previously observed in percolation.

As a proposal for future work, it would be to extend to lattices of larger dimensions and to a larger number of tries of the global sum rule the detailed study that was made for 2 dimensions. In particular it will be relevant to determine the critical point r_c, determine in which conditions there are two or one or none crossing points and apply finite-size scaling when appropriate. One could also analyze if there are significant changes in other characteristics of the transition.

In view of what has been reviewed in the bibliography, and the differences that can be observed between site percolation and bond percolation, as well as between the sum and product rule, it would be interesting to test the algorithm using the product instead of the sum, and also bond percolation.

We consider that this is a subject that needs to be explored in more detail to understand and classify the transition and to be able to address its applications. As briefly commented in the first section of the work, mastering this type of systems is great importance and usefulness in future applications, therefore it would be interesting and a great challenge to develop a strict theoretical analysis.

References

[1] Dimitris Achlioptas, Raissa M D'Souza, and Joel Spencer. Explosive percolation in random networks. *Science*, 323(5920):1453–1455, 2009.

[2] Vinod KS Shante and Scott Kirkpatrick. An introduction to percolation theory. *Advances in Physics*, 20(85):325–357, 1971.

[3] Geoffrey Grimmett. What is percolation? In *Percolation*, pages 1–31. Springer, 1999.

[4] Dietrich Stauffer and Ammon Aharony. *Introduction to percolation theory*. CRC press, 2018.

[5] Nikolaos Bastas, Paraskevas Giazitzidis, Michael Maragakis, and Kosmas Kosmidis. Explosive percolation: Unusual transitions of a simple model. *Physica A: Statistical Mechanics and its Applications*, 407:54–65, 2014.

[6] Raissa M D'Souza, Jesus Gómez-Gardeñes, Jan Nagler, and Alex Arenas. Explosive phenomena in complex networks. *Advances in Physics*, 68(3):123–223, 2019.

[7] Raissa M D'Souza and Jan Nagler. Anomalous critical and supercritical phenomena in explosive percolation. *Nature Physics*, 11(7):531–538, 2015.

[8] Simon R Broadbent and John M Hammersley. Percolation processes: I. crystals and mazes. In *Mathematical Proceedings of the Cambridge Philosophical Society*, volume 53, pages 629–641. Cambridge University Press, 1957.

[9] Deokjae Lee, Young Sul Cho, and Byungnam Kahng. Diverse types of percolation transitions. *Journal of Statistical Mechanics: Theory and Experiment*, 2016(12):124002, 2016.

[10] Kurt Binder. Theory of first-order phase transitions. *Reports on progress in physics*, 50(7):783, 1987.

[11] H Eugene Stanley, José S Andrade Jr, Shlomo Havlin, Hernán A Makse, and Béla Suki. Percolation phenomena: a broad-brush introduction with some recent applications to porous media, liquid water, and city growth. *Physica A: Statistical Mechanics and its Applications*, 266(1-4):5–16, 1999.

[12] P Agrawal, S Redner, PJ Reynolds, and HE Stanley. Site-bond percolation: a low-density series study of the uncorrelated limit. *Journal of Physics A: Mathematical and General*, 12(11):2073, 1979.

[13] Paul Erdős and Alfréd Rényi. On the evolution of random graphs. *Publ. Math. Inst. Hung. Acad. Sci*, 5(1):17–60, 1960.

[14] Filippo Radicchi and Santo Fortunato. Explosive percolation: A numerical analysis. *Physical Review E*, 81(3):036110, 2010.

[15] PL Leath. Cluster size and boundary distribution near percolation threshold. *Physical Review B*, 14(11):5046, 1976.

[16] Z Alexandrowicz. Critically branched chains and percolation clusters. *Physics Letters A*, 80(4):284–286, 1980.

[17] Joseph Hoshen and Raoul Kopelman. Percolation and cluster distribution. i. cluster multiple labeling technique and critical concentration algorithm. *Physical Review B*, 14(8):3438, 1976.

[18] Mark EJ Newman and Robert M Ziff. Fast monte carlo algorithm for site or bond percolation. *Physical Review E*, 64(1):016706, 2001.

[19] MEJ Newman and Robert M Ziff. Efficient monte carlo algorithm and high-precision results for percolation. *Physical Review Letters*, 85(19):4104, 2000.

[20] Tom Bohman and Alan Frieze. Avoiding a giant component. *Random Structures & Algorithms*, 19(1):75–85, 2001.

[21] Nikolaos Bastas, Kosmas Kosmidis, and Panos Argyrakis. Explosive site percolation and finite-size hysteresis. *Physical Review E*, 84(6):066112, 2011.

[22] Kurt Binder. Critical properties from monte carlo coarse graining and renormalization. *Physical Review Letters*, 47(9):693, 1981.

[23] Nuno AM Araujo and Hans J Herrmann. Explosive percolation via control of the largest cluster. *Physical review letters*, 105(3):035701, 2010.

[24] Zhu Yong, Yang Zi-Qing, Zhang Xin, and Chen Xiao-Song. Critical behaviors and universality classes of percolation phase transitions on two-dimensional square lattice. *Communications in Theoretical Physics*, 64(2):231, 2015.